Review

Supercapatteries as Hybrid Electrochemical Energy Storage Devices: Current Status and Future Prospects

Subarna Rudra , Hyun Woo Seo , Subrata Sarker * , Dong Min Kim *

Posted Date: 6 December 2023

doi: 10.20944/preprints202312.0355.v1

Keywords: electrochemical energy storage; supercapacitors; batteries; hybrid storage; supercapatteries

Review

Supercapatteries as Hybrid Electrochemical Energy Storage Devices: Current Status and Future Prospects

Subarna Rudra, Hyun Woo Seo, Subrata Sarker *and Dong Min Kim *

Department of Materials Science and Engineering, Hongik University, Sejong, Korea
* Correspondence: subrata_sarker@yahoo.com (S.S.); dmkim@hongik.ac.kr (D.M.K.)

Abstract: Among the electrochemical energy storage (EES) technologies, rechargeable batteries (RBs) and supercapacitors (SCs) are the two most desired candidates for powering a range of electrical and electronic devices. The RB operates on Faradaic processes, whereas the underlying mechanisms of the SC vary as non-Faradaic in the electrical double layer capacitors (EDLCs), Faradaic at the surface of the electrodes in the pseudo capacitors (PCs), and a combination of both non-Faradaic and Faradaic in the hybrid capacitors. The EDLCs offer high power density but low energy density. The hybrid capacitors take advantage of the Faradaic process without compromising their capacitive nature. Unlike batteries, supercapacitors provide high power density and numerous charge-discharge cycles; however, their energy density lags that of batteries. Here, we review recently published critically selected articles on supercapatteries, a generic term that refers to EES devices that can combine the merits of EDLCs and RBs. Also discussed are the properties, design strategies, and future perspectives of supercapatteries.

Keywords: electrochemical energy storage; supercapacitors; batteries; hybrid storage; supercapatteries

1. Introduction

Our earth's climate is changing primarily due to anthropogenic global warming, which is attributed to the burning of Fossil Fuels. It will continue to change at that pace or even more quickly until we take corrective measures [1]. Fortunately, we have started acknowledging the negative impacts of climate change on our environment [2]. As such, the major world powers and the scientific community have focused on renewable energy to curb fossil fuels, a primary culprit of climate change. Since renewable energies are intermittent energy sources, they require energy storage devices to maintain a steady supply. Recently, electric vehicles (EVs) have become increasingly popular as they are not an active source of carbon emissions and depend on an electric grid or solar array at an invariable or reduced cost. As a result, there has been a great interest in developing efficient electrochemical energy storage (EES) devices.

Among EES technologies, rechargeable batteries (RBs) and supercapacitors (SCs) are the two most desired candidates for powering a range of electrical and electronic devices [3–10]. The RBs operate on Faradaic processes, whereas the underlying mechanism of the SCs varies as non-Faradaic at the electrical double layer capacitors (EDLCs), Faradaic at the surface of the electrodes in the pseudocapacitors (PCs), and a combination of both non-Faradaic and Faradaic in the hybrid SCs (HSCs) [3]. The EDLCs offer high power density but low energy density. The HSCs take advantage of the Faradaic process without compromising their capacitive nature. Unlike batteries, supercapacitors provide high power density and numerous charge-discharge cycles; however, they lag batteries in energy density. To take advantage of the merits of both RBs and SCs, researchers have focused on merging the two technologies into a single device known as "supercapattery" (= **supercapa**citor + ba**ttery**) [11–15], a generic term used to identify a unique category of energy storage devices that offer high energy density like an RB without compromising the ability to deliver high power density and large cyclability of EDLC. Though supercapatteries are relatively new compared to RBs and SCs, supercapatteries have received significant attention, as evidenced by the exponential growth of related publications over the past ten years (Figure 1). The advantage of supercapatteries

Preprints (www.preprints.org) | NOT PEER-REVIEWED | Posted: 6 December 2023 doi:10.20944/preprints202312.0355.v1

over other EES is evident in the Ragone plots in Figure 2, which compare the power and energy densities of several typical EES systems. However, it is often difficult to distinguish between supercapatteries and other hybrid EES devices due to their overlapping properties.

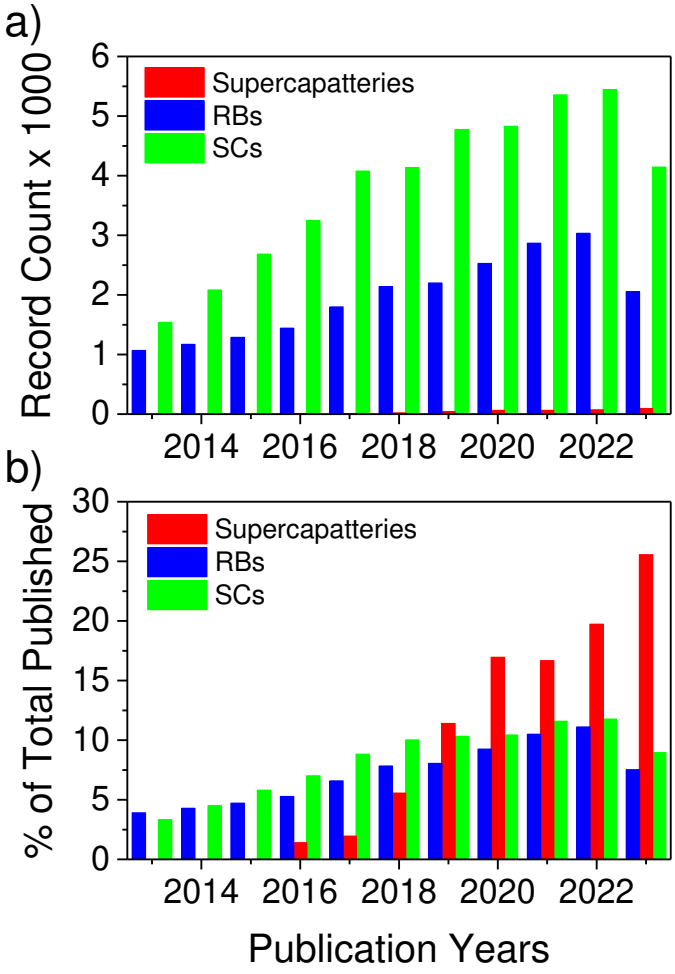

Figure 1. a) Number of articles and b) percent of total number of articles published on supercapatteries, rechargeable batteries (RBs), and supercapacitors (SCs) over the last ten years (from 2013 to 2023).

Preprints (www.preprints.org) | NOT PEER-REVIEWED | Posted: 6 December 2023 doi:10.20944/preprints202312.0355.v1

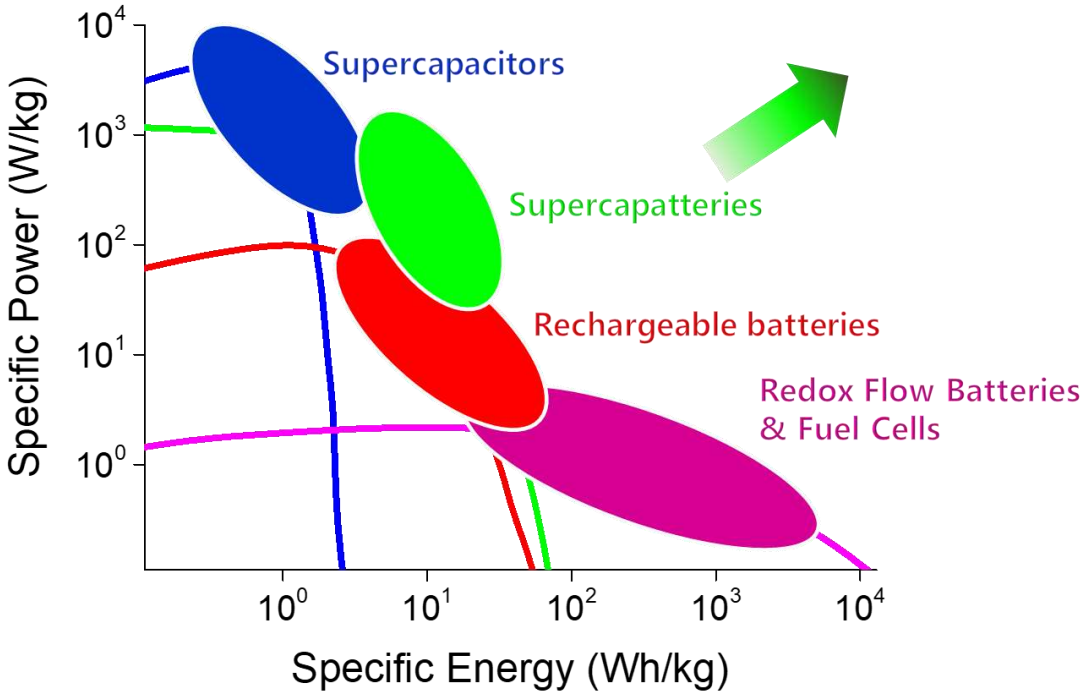

Figure 2. Ragone plot of different energy storage devices showing relative energy and power density for supercapacitors, rechargeable batteries, redox flow batteries, fuel cells, and supercapatteries [15].

Here, we review selected articles on supercapatteries encompassing characteristics of RBs and SCs with high-energy and high-power densities, respectively. The review discusses different types of electrochemical energy storage devices in terms of mechanisms and materials to form a supercapattery. The properties and the design strategies of supercapatteries, along with their electrochemical characterization, are also discussed. The final section summarizes the review with a perspective of supercapatteries in the future.

2. Some Important Definitions and Parameters of EES

2.1. Capacitance and Charge of an Electrode

The capacitance (C) of a dielectric capacitor depends on the area (A) of the conducting electrodes and the distance (d) between the electrodes as

$$C = \frac{\varepsilon_r \varepsilon_0 A}{d} \quad (1)$$

where ε_r and ε_0 are the relative and vacuum permittivity, respectively. According to Eq. (1), the capacitance of the EDLCs increases as A increases and d decreases. The behavior of an electrode/electrolyte interface is analogous to that of a capacitor. At a voltage (V) across the capacitor with a capacitance of C, the total amount of charge (Q) stored is [16]

$$Q = CV \quad (2)$$

When two capacitors with capacitance C_1 and C_2 are connected in series, their total capacitance (C_T) is expressed as

$$\frac{1}{C_T} = \frac{1}{C_1} + \frac{1}{C_2} \quad (3)$$

If C_1 and C_2 are the same, that is, $C_1 = C_2 = C$, then Eq. (3) becomes.

Preprints (www.preprints.org) | NOT PEER-REVIEWED | Posted: 6 December 2023 doi:10.20944/preprints202312.0355.v1

$$C_T = \frac{C}{2} \quad (4)$$

However, if the two capacitors are different and C_1 is much smaller than C_2 ($C_1 \ll C_2$), then $C_1 + C_2 \cong C_2$ and Eq. (3) becomes

$$C_T \cong C_1 \quad (5)$$

That is, the total capacitance of a series combination of two capacitors with different capacitances will be dominated by the capacitor with a smaller capacitance.

Moreover, differentiating Eq. (2) with respect to time (t) gives Eq. (7).

$$\frac{dQ}{dt} = C\frac{dV}{dt} + V\frac{dC}{dt}, \quad (6)$$

Since $i = dQ/dt$ and considering C does not change with time, Eq. (7) can be written as [17]

$$C = \frac{dQ}{dt}/\frac{dV}{dt} = i/\frac{dV}{dt}, \quad (7)$$

which can be written for $v = dV/dt$ as

$$C = \frac{i}{v} \quad (8)$$

2.2. Galvanostatic charge-discharge (GCD)

In the Galvanic technique, voltage response is measured by applying a constant current within a potential window bounded by initial and final voltages. Galvanostatic charge-discharge (GCD) is one of the most effective techniques to evaluate the capacity and capacitance of RBs and SCs at a constant current. According to Eq. (7), during the charging process of a capacitor at a constant current, the voltage increases at a constant rate. Conversely, during the discharging process, the voltage decreases at a constant rate. This results in a triangular curve in GCD, as depicted in Figure 3a [18]. Thus, one can calculate the capacitance of an electrode material from the discharge current (i) and the slope (dV/dt) of the discharging part of the triangular GCD curve [19].

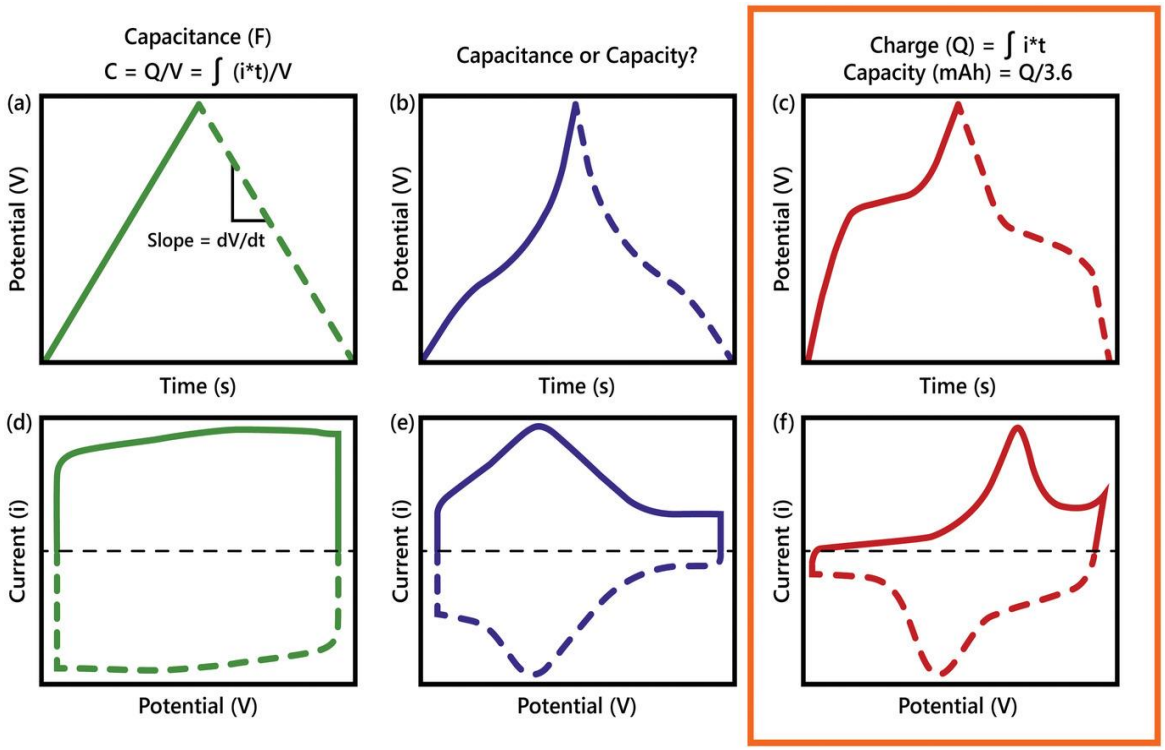

Preprints (www.preprints.org) | NOT PEER-REVIEWED | Posted: 6 December 2023 doi:10.20944/preprints202312.0355.v1

Figure 3. Archetypal electrical output behavior of three main types of electrodes, including a,d) electrical double layer, b, e) pseudocapacitive, and c,f) battery type. a–c) Schematic of galvanostatic charge-discharge (GCD) profiles showing linear and nonlinear responses with time and d–f) corresponding cyclic voltammetry (CV) profiles [23].

2.3. Cyclic Voltammetry (CV)

Cyclic voltammetry (CV) is one of the most popular electrochemical techniques for investigating new electrochemical systems or materials. In CV measurement, a linear potential sweep or ramp is applied where the potential (V, V) is changed from an initial value V_i (V) as [20]

$$V = V_i + \nu t \tag{9}$$

Therefore, the current flowing through a capacitor is in a linear relationship with ν but independent of V. For a constant C, Eq. (8) gives the rectangular *i-V* plots as shown in Figure 3d. However, CV plots for pseudocapacitive and faradaic electrodes are not linear, as shown in Figure 3e-f. Analysis of the CV profile or voltammogram can provide several useful information, including the cyclability of the process, the total capacitance, the optimum potential window, the electrochemical kinetics of electrodes, and an ability to distinguish the capacitive and diffusion-limited charge storage mechanisms by altering the sweep rate [18]. The capacitance of the electrodes under study can be estimated by integrating the CV curves according to Eq. (10) [19].

$$c = \frac{\int_{V_1}^{V_2} i dV}{\nu \Delta V}, \tag{10}$$

where i is the discharge current, i.e., the current below the X axis, ν is the scan rate, and $\Delta V = V_2 - V_1$ is the operating discharge potential range.

2.4. Electrochemical impedance spectroscopy (EIS)

Electrochemical impedance spectroscopy (EIS) is a powerful method for characterizing the electrical properties of materials and their interfaces. In EIS, a small amplitude modulated voltage $V(\omega, t)$ is applied over a wide range of frequencies ($f = \omega/2\pi$) and the corresponding currents $i(\omega, t)$ are recorded, or vice versa. The resultant impedance $Z(\omega)$ of the system is calculated as [21]

$$Z(\omega) = \frac{V(\omega, t)}{i(\omega, t)} \tag{11}$$

The impedance is often represented by the real part Z' and imaginary part Z'' as a complex number.

$$Z = Z' + jZ'' \tag{12}$$

A detailed account of electrochemical impedance and complex capacitance to interpret electrochemical capacitors was given by Itagaki et al.[22]. Like complex impedance, complex capacitance can also be expressed as

$$C = C' + jC'' \tag{13}$$

The relationship between Eq. (12) and Eq. (13) is defined by $C = 1/j\omega Z$, where $C' = -Z''/\omega(Z'^2 + Z''^2)$ and $C'' = -Z'/\omega(Z'^2 + Z''^2)$.

Figure 5 shows typical EIS spectra in complex plane distinguishing different charge storage mechanisms [23].

Preprints (www.preprints.org) | NOT PEER-REVIEWED | Posted: 6 December 2023 doi:10.20944/preprints202312.0355.v1

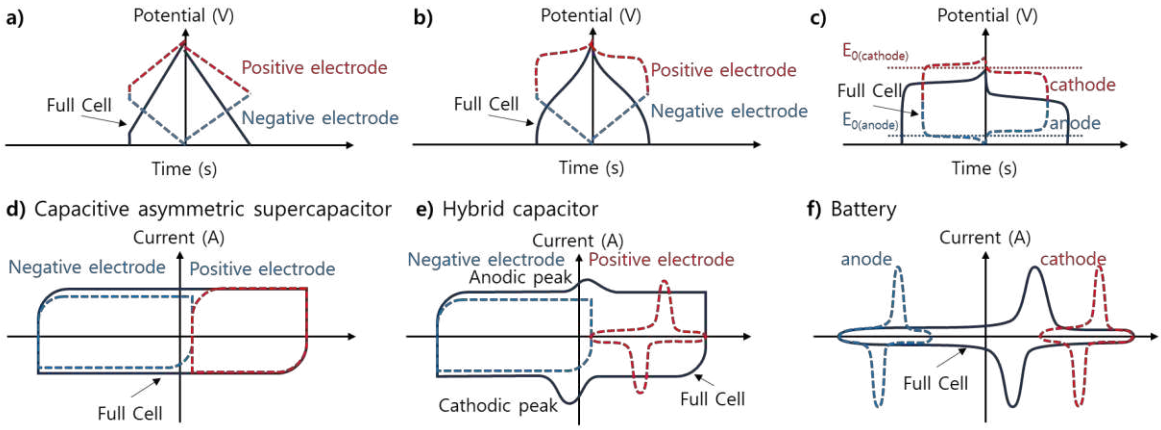

Figure 4. Schematic illustration of the typical GCD (up) and CV (bottom) curves depicting characteristics of (a and d) a capacitive asymmetric supercapacitor, (b and e) a hybrid capacitor, and (c and f) a battery [53].

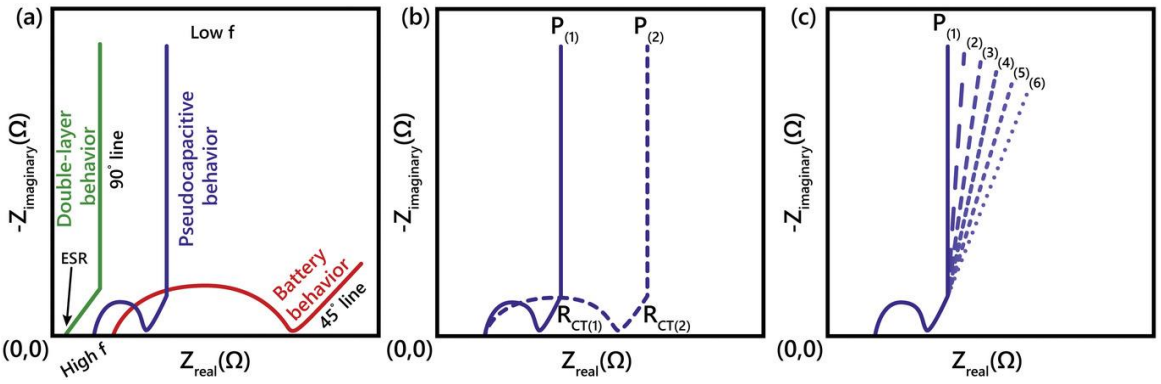

Figure 5. a) Typical Nyquist plot representations for an EDLC (green curve), pseudocapacitive materials (blue) and battery (red). ESR, 45° and 90° lines0020are marked, b) Example spectra of confirming real charge transfer resistance (RCT) by doing EIS at two different potentials (solid and dotted blue curves), in contrast to c) where interfacial impedance would lead to constant RCT at all potentials. Pseudocapacitive materials will show minimal diffusion-limited behavior (meaning no diffusion limitations relative to batteries)[23].

2.5. Energy Density

The electric energy stored in SCs, i.e., the energy density (E, Wh/kg), can be evaluated by integrating the GCD curves. For EDLCs and PCs with linear GCD curves, the integration turns into the calculation of triangle areas, as shown in Figure 4d; therefore, the energy density can be calculated by [19]

$$E = \int QdV = \int_0^V CVdV = \frac{1}{2}CV^2 \quad (14)$$

However, in the case of HSC with a nonlinear GCD curve, as shown in Figure 4e, the energy density cannot be calculated simply by using Eq. (14) due to the nonlinear change of V. In this case, energy density should be calculated following Eq. (15).

$$E = \int QdV = \int_{t_1}^{t_2} iV_t dt = \frac{1}{2}CV^2 \quad (15)$$

Preprints (www.preprints.org) | NOT PEER-REVIEWED | Posted: 6 December 2023 doi:10.20944/preprints202312.0355.v1

Eq. (15) considers all discharge times (t_{dischage}) in hour (h), and discharge voltages (V_t) for the calculation after the initial IR drop. In Eq. (15), t_1 is the time after the initial IR drop, t_2 is the moment that the discharge is finished, and i is the constant current applied to the supercapacitor.

2.6. Power density

The power density (P, W/kg) values of SCs can be calculated according to Eq. (16)[24]

$$P = \frac{E}{t}, \tag{16}$$

where t is the discharge time in hour (h).

2.7. Notation for Electrodes of EES

Several terms have often been used interchangeably in EES to denote electrodes like positrode for the positive electrode and negatrode for the negative electrode, since G. Z. Chen proposed those terms in 2015 to avoid any confusion among the newcomers to the EES community [17]. It is important to note that the terms cathode or anode are not always suitable for EES as EDLCs are non-Faradaic and capacitive.

3. Electrochemical Energy Storage (EES) Devices

Batteries and capacitors are the two types of energy storage devices relevant to EES devices [25]. Essentially, batteries are non-rechargeable (primary cell) and rechargeable (RBs, secondary cell). On the other hand, capacitors are of three types – non-electrolytic, electrolytic, and electrochemical or supercapacitors (SCs). The EES devices comprise RBs, SCs, and their derivatives. The EES devices are different in that these devices store energy following different storage mechanisms – non-Faradaic (surface-controlled kinetics) and Faradaic (diffusion-controlled kinetics) – that depend on the materials (electrode and electrolyte) and how those materials are used in the device [8,23].

Figure 6 illustrates three charge storage mechanisms and how those differentiate SCs from RBs. In a non-Faradaic process, the charge accumulation occurs electrostatically by opposite charges residing on two interfaces separated by a vacuum (non-electrolytic) or a molecular dielectric (electrolytic). In contrast, in a Faradaic process, a redox reaction achieves the same, causing chemical or oxidation state changes in the electroactive materials [3,25]. The Faradaic process can be capacitive (pseudocapacitive), as in PCs, and non-capacitive, as in batteries [18]. Before diving into supercapatteries, understanding three main EES – EDLCs, PCs, and RBs – is essential, as shown in Figure 6. The charge storage mechanisms in those devices can be well understood by their electrochemical signature in cyclic voltammetry (CV) and galvanostatic charge/discharge (GCD) profiles (Figure 3). Mathis et al. outlined a set of guidelines for interpreting the performance of EES systems [23]. An EDLC material will show a linear voltage versus time response (a triangular-shaped GCD profile) during constant current charging/discharging (Figure 3a) and a rectangular CV profile or cyclic voltammogram (Figure 3d). In this case, the amount of charge stored depends linearly on potential, and the capacitance of the material can be easily calculated and reported for the EDLC. On the other hand, an RB material will show plateaus in the GCD profile (Figure 3c) and separated oxidative and reductive peaks in the CV profile (Figure 3f). Unlike the case of charge storage at EDLC electrodes, charge storage by RB-type electrodes follows a nonlinear relationship with the applied potential. In the case of pseudocapacitive materials, the GCD profile (Figure 3b) is symmetric but non-linear, and the CV response (Figure 3e) does not separate the oxidative and reductive peaks.

Preprints (www.preprints.org) | NOT PEER-REVIEWED | Posted: 6 December 2023 doi:10.20944/preprints202312.0355.v1

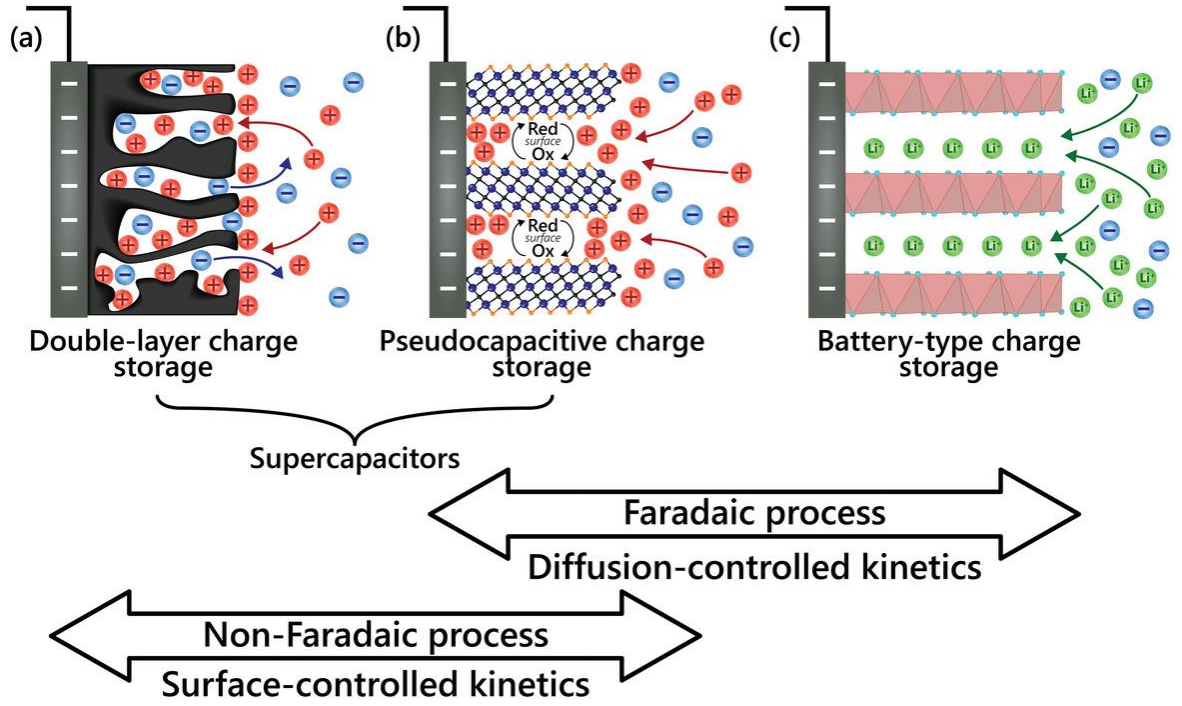

Figure 6. Illustration of the electrode processes occurring at a) electrical double layer capacitive, b) pseudocapacitive, and c) Faradaic electrodes [23].

3.1. Supercapacitors (SCs)

Depending on the storage mechanism, SCs can be classified mainly into three categories: EDLCs, PCs, and a combination of the two as HSCs [17,26–28] or Asymmetric SCs (ASCs)[18,19,29], where HSCs are the subset of ASCs. Another way of differentiating ASCs from HSCs is that ASCs are configured by combining the electrode materials of EDLCs and PCs. In contrast, HSCs combine the electrode materials of EDLCs and RBs [30].

3.1.1. Electrical Double Layer Capacitors (EDLCs)

Like conventional dielectric capacitors, EDLCs store energy electrostatically, forming an electrical double layer (EDL) at the electrode/electrolyte interfaces, where the applied voltage polarizes the electrolyte that acts as a dielectric (Figure 7) [16,17,31,32]. The process is purely non-Faradaic and physical in nature. Thus, Eq. (1) applies to EDLCs, and the charging-discharging mechanism of EDLCs is very fast and reversible. Also, EDLCs primarily utilize carbonaceous materials like activated carbon (AC), graphene, carbon nanotubes (CNTs), carbon-aerogel (CA), carbide-derived carbon (CDC), carbon fibers, etc. [33] The capacitance of EDLCs mostly depends on the pore size of the electrode materials. Because of the porous electrodes with large surface areas that allow the formation of compact double layers with atomic range separation between electronic and ionic charges at the electrode surface, EDLCs show greater capacitance than conventional dielectric capacitors [31,33].

Preprints (www.preprints.org) | NOT PEER-REVIEWED | Posted: 6 December 2023 doi:10.20944/preprints202312.0355.v1

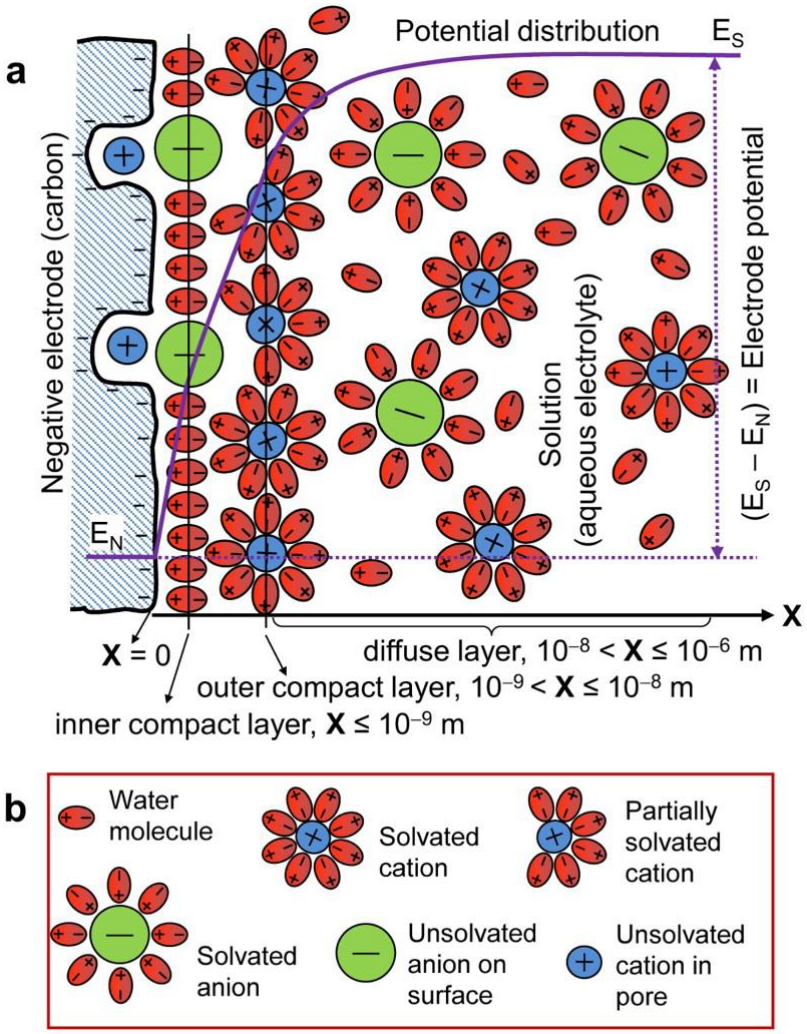

Figure 7. Schematic representations of a) the EDL structure (cross-section) of the interface between a porous carbon negative electrode and an aqueous electrolyte; b) explanations of symbols in a) [16,17].

3.1.2. Pseudocapacitors (PCs)

In PCs, energy is stored via a sequence of fast reversible processes, which are Faradaic in nature, at the surface or near-surface of the electrode materials [8,34–36]. Conway identified three different Faradaic mechanisms, including underpotential deposition, electrosorption, and intercalation, that cause pseudocapacitance, as shown in Figure 8 [34,37]. In underpotential deposition, metal ions form an adsorbed monolayer at the surface of a different metal well above their redox potential. An example of such an underpotential deposition is the deposition of lead (Pb) on the surface of a gold (Au) electrode (Figure 8a) [38]. Redox pseudocapacitance occurs when ions are electrochemically adsorbed onto the surface or near the surface of a material following a Faradaic charge-transfer process (Figure 8b). Intercalation pseudocapacitance occurs when ions intercalate into the layers of a redox-active material in a Faradaic charge-transfer process without changing the crystallographic phase (Figure 8c) [34].

Preprints (www.preprints.org) | NOT PEER-REVIEWED | Posted: 6 December 2023 doi:10.20944/preprints202312.0355.v1

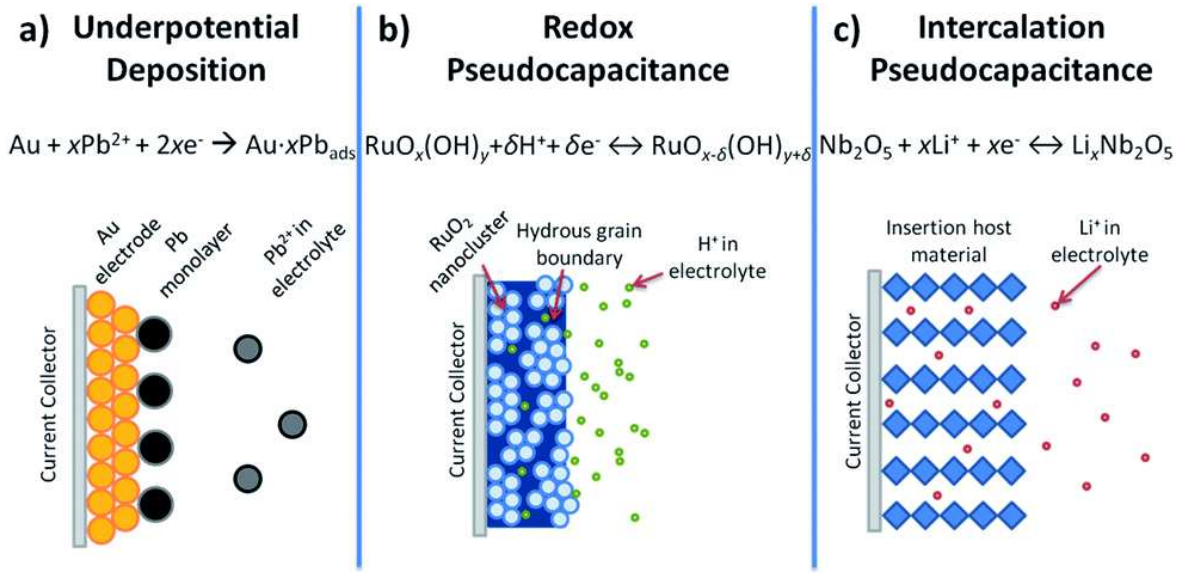

Figure 8. Different types of reversible redox mechanisms that cause pseudocapacitance: a) underpotential deposition, b) redox pseudocapacitance, and c) intercalation pseudocapacitance [34].

The above three Faradaic processes occur due to different physical processes involving various types of materials that result in similar electrochemical signatures owing to the relationship between potential and the extent of charge developed from adsorption/desorption processes at the electrode/electrolyte interface [34]:

$$E \sim E^0 - \frac{RT}{nF} \ln\left(\frac{X}{1-X}\right), \tag{16}$$

where E is the potential, R is the ideal gas constant, T is the temperature, n is the number of electrons, F is the Faraday constant, and X is the extent of fractional coverage of the surface or inner structure. From Eq. (16), a capacitance (C) may be defined in regions where the plot of E vs. X is linear:

$$C = \frac{nF}{m}\frac{X}{E}, \tag{17}$$

where m is the molecular weight of the active material. The capacitance, C, is not always constant since the plot of E vs. X is not entirely linear as in a capacitor, and so it is termed pseudocapacitance [34].

There are detailed reviews on PCs and related pseudocapacitive materials [33,35,36,39]. Electrode materials that are used in PCs are transition-metal oxides (TMOs) such as IrO_2, RuO_2, Fe_3O_4, MnO_2, NiO, V_2O_5, Co_3O_4 etc.; transition-metal sulfides (TMSs) such as MoS_2, WS_2, FeS_2; and conducting polymers (CPs) such as polyaniline (PANI), polythiophene, polypyrrole (PPy), polyvinyl alcohol (PVA), poly (3,4-ethylene dioxythiophene) (PEDOT), polyacetylene, poly (4-styrene sulfonate) (PSS), poly-phenylene-vinylene (PPV), etc. [33,40]. Recently, many nanomaterials have been introduced to RBs that showed fast redox kinetics comparable to pseudocapacitive materials due to very short ionic diffusion length and high surface area of the nanosized materials. As a result, pseudocapacitive and battery materials are becoming increasingly indistinguishable [36]. According to Brousse et al., some materials are described as "pseudocapacitive" materials even though their electrochemical signature is analogous to that of a "battery material," as commonly observed for $Ni(OH)_2$ in KOH electrolyte. In contrast, true pseudocapacitive electrode materials such as MnO_2 display electrochemical behavior typical of that observed for a capacitive carbon electrode [41]. Faradaic electrodes exhibit electrochemical behavior distinct from that of pseudocapacitive electrodes. So, they proposed that the term "pseudocapacitive" must be only used to describe electrode materials (e.g., MnO_2) that display an electrochemical behavior typical of that observed for

Preprints (www.preprints.org) | NOT PEER-REVIEWED | Posted: 6 December 2023 doi:10.20944/preprints202312.0355.v1

a capacitive carbon electrode in a mild aqueous electrolyte to avoid any confusion between battery materials and pseudocapacitive materials.

3.1.3. Hybrid supercapacitors (HSCs)

Hybrid SCs (HSCs) combine the best of EDLCs with the best of PCs or RBs into a single device in different combinations of electrode materials and storage mechanisms (non-Faradaic and Faradaic) (Figure 9) [18,19,42]. Hybridizing different electrode materials into a single electrode or fabricating a hybrid cell configuration consisting of Faradaic and non-Faradaic electrodes has become an obvious strategy for developing high-energy and high-power HSCs [8]. Thus, asymmetry in HSCs may arise from electrode materials and storage mechanisms. These devices take advantage of the fast kinetics of EDLC materials and the improved energy storage performance of pseudocapacitive or battery electrode materials [36]. Schematic illustrations of electrochemical profiles (CV and GCD curves) of a capacitive asymmetric supercapacitor (different non-Faradaic materials) and a hybrid capacitor (non-Faradaic and Faradaic materials) are shown in Figure 4a,d, and Figure 4b,e, respectively.

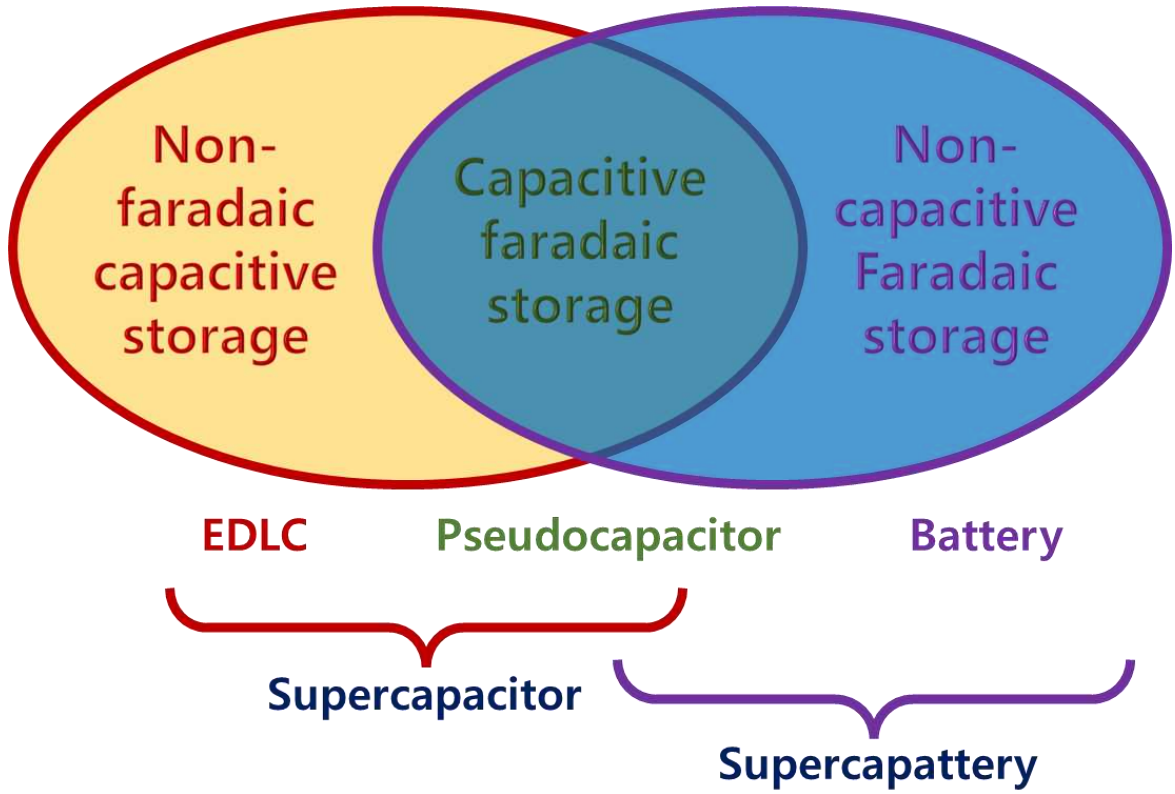

Figure 9. Schematic correlation between EDL capacitor, pseudocapacitor, battery, and supercapattery according to charge storage processes [18].

3.2. Rechargeable batteries (RBs)

Like most electrochemical devices, RBs are composed of two electrodes – a cathode and an anode – separated by an electrolyte [4,43–45]. In RBs, electrical energy is converted and stored electrochemically within the bulk of the electrodes through reversible chemical reactions at the electrode/electrolyte interfaces during the charging and discharging processes. There are various kinds of RBs; among them, lithium (Li)-ion batteries (LiBs), a type of metal-ion battery, are the most commercially successful RB technology [4,43].

The emergence of LiBs, a Nobel prize-winning and one of the most popular EES technologies in the nineties, has revolutionized consumer electronics and EVs [4,7,46,47]. Typically, LiBs comprise five key components – anode, cathode, electrolyte, separator, and current collectors – as shown in Figure 10 [4]. Generally, copper (Cu) and aluminum (Al) foils are used as current collectors at the

Preprints (www.preprints.org) | NOT PEER-REVIEWED | Posted: 6 December 2023 doi:10.20944/preprints202312.0355.v1

anode and cathode. The negative electrode (anode) is made of carbonaceous materials (e.g., graphite), whereas Li-based metal oxides (e.g., $LiCoO_2$) are used in the positive electrode (cathode). Other materials used in the anode are germanium-based materials, transition metal chalcogenides, silicon, and metallic oxides [48]. The two electrodes are separated by a separator, typically a porous polyolefin film soaked in a non-aqueous solution of a lithium salt (e.g., $LiPF_6$ in ethylene carbonate, ethyl methyl carbonate, or diethyl carbonate) [4,43]. In LiBs, the reversible chemical reaction occurs in two ways: displacement and insertion in the electrodes [4]. During the charging cycle, the positive electrolyte ions (Li^+) are deintercalated (displaced) from the cathode and intercalated (inserted) into the anode. The reverse process occurs during the discharging cycle, where the positive ions transport from the anode to the cathode, and electrons travel from the anode to the cathode via an external load and thereby complete the circuit (Figure 11a). This displacement/insertion process involves reversible Faradaic processes that can be identified as well-separated oxidative and reductive peaks in the CV profile (Figure 11b) and asymmetric curves in the GCD profile (Figure 11c, d). Emerging RBs based on abundant alkali, alkaline earth, and transition metals – sodium (Na), potassium (K), magnesium (Mg), calcium (Ca), zinc (Zn), and aluminum (Al) – are promising alternatives to LiBs [6,45]. Figure 4c,f illustrates the CV and GCD profiles of an RB.

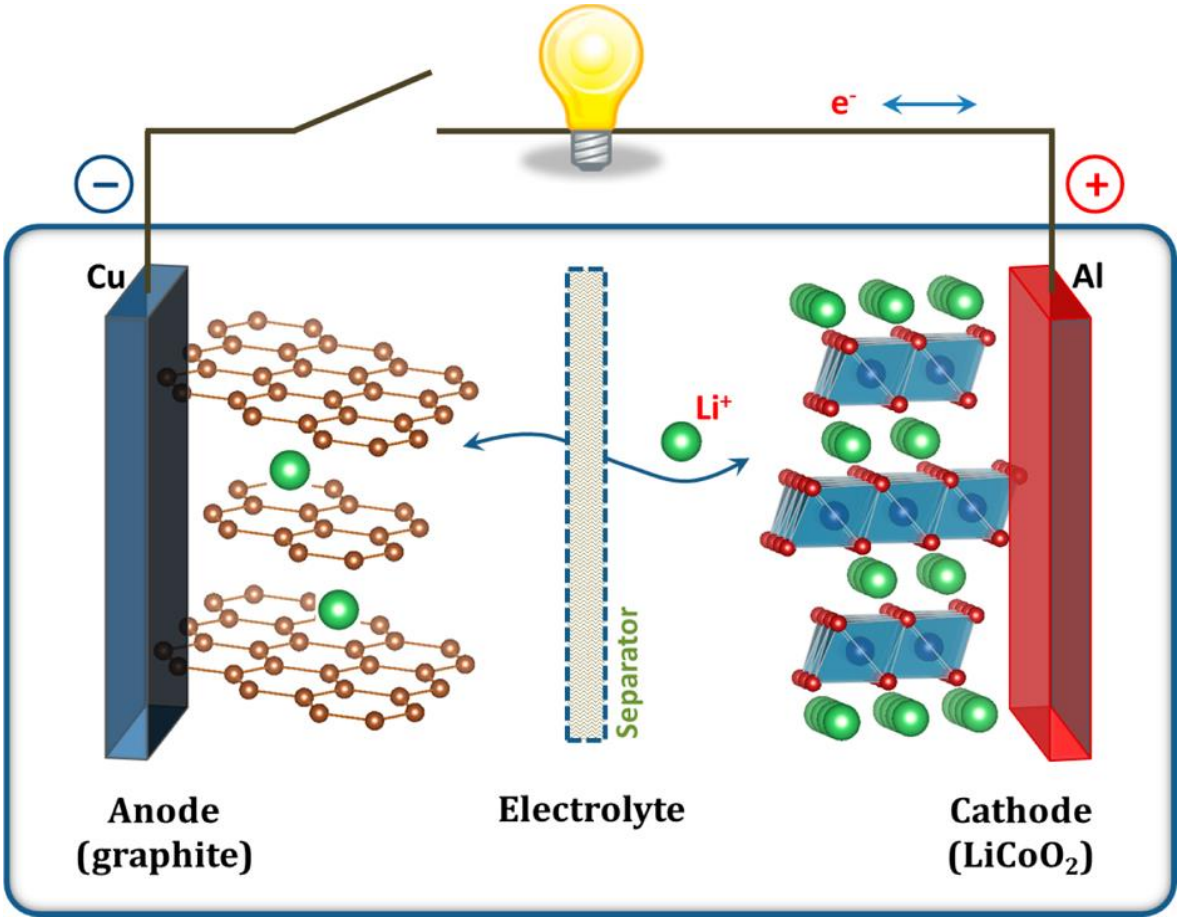

Figure 10. Schematic illustration of the first Li-ion battery ($LiCoO_2$/Li^+ electrolyte/graphite) [4].

Preprints (www.preprints.org) | NOT PEER-REVIEWED | Posted: 6 December 2023 doi:10.20944/preprints202312.0355.v1

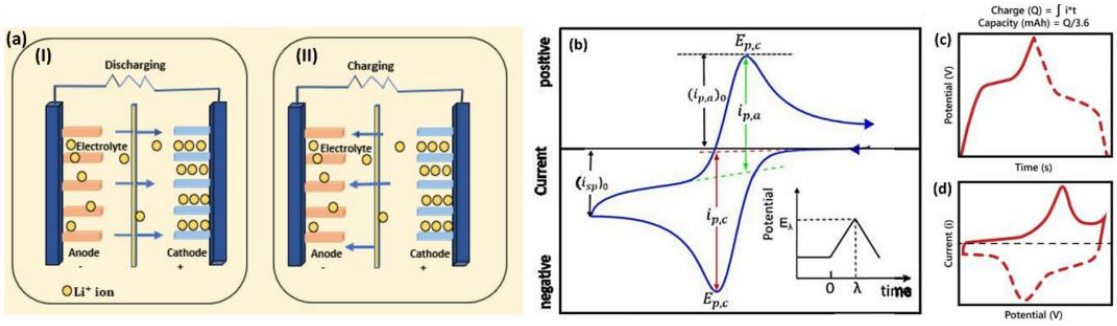

Figure 11. Schematic diagram of a) charge storage mechanism: (i) charging and (ii) discharging, b) cyclic voltammogram (CV), and (c, d) galvanostatic charge-discharge (GCD) curves of LiBs [15].

3.3. Supercapatteries

Supercapatteries are hybrid EES devices that combine the advantages of SCs and RBs, such as high energy density, high power density, and long cycle life. This EES hybrid design involves a combination of an SC electrode with an RB electrode, such as the so-called Li-ion capacitor [49–51], Na-ion capacitors [50,52], and other hybrid EES devices [14]. Supercapatteries can exhibit capacitive performances like conventional capacitors, including CV and linear GCD profiles. Thus, the fundamentals of conventional capacitors can also be applied to supercapatteries in which capacitance (C) is the ratio of the change of stored charge (ΔQ) to the variation in applied voltage (ΔV) as the voltage of a capacitor is swept at a constant voltage scan rate ($\nu = \frac{dU}{dt}$) in CV. Because current (i) flowing through a capacitor is proportional to ν, this proportionality is also equal to C, as described in Eq. (18)[14].

$$C = \frac{\Delta q}{\Delta U} = \frac{dq/dt}{dU/dt}, \tag{18}$$

which is essentially the same as Eq. (7). Figure 4b,e show the schematic of electrochemical profiles, including CV and GCD curves of typical supercapatteries. Another term often used along with supercapattery is "supercabattery," which performs more like an RB but with higher power capability and/or longer charge-discharge durability [53–56]. Table 1 shows how different combinations of electrode materials with varying mechanisms of storage give rise to supercapatteries [17].

Table 1. Ways of pairing the same or different electrode materials into supercapacitor, battery, supercapattery or supercabattery [17.].

Device			**Supercapattery**						**Battery**
	Supercapacitor					**Hybrid**		Supercabattery	
	EDLC		**Pseudocapacitor**						
Electrode Material	**NFCS**	**NFCS**	**NFCS**	**CFS**	**CFS**	**NFCS**	CFS	NCFS	NCFS
	1+1	1+2	1+3	1+1	1+2	1+3	1+1	1+1	1+2
	NFCS	NFCS	CFS	CFS	CFS	NCFS	NCFS	NCFS	NCFS

NFCS: **N**on-**F**aradaic **C**apacitive **S**torage (EDLC storage); **CFS:** **C**apacitive **F**aradaic **S**torage (Pseudocapacitive storage); **NCFS:** **N**on-**C**apacitive **F**aradaic **S**torage (Battery-type storage); **1+1:** Symmetrical device of the same electrode material; **1+2:** Asymmetric device of different materials with the same storage mechanism; **1+3:** Asymmetrical device of different materials with different storage mechanisms.

 doi:10.20944/preprints202312.0355.v1

3.3.1. Electrode and Electrolyte Materials of Supercapatteries

Different supercapatteries can be fabricated utilizing electrodes with capacitive, pseudocapacitive, or battery-type materials. To comprehensively discuss these hybrid devices, Liu and Chen constructed several hypothetical supercapatteries to illustrate their performance by using corresponding GCD plots one by one (Figure 12a–d), and these hypothetical devices were confirmed by using relevant experimental data from the literature (Figure 12e–h)[14]. Table 2 summarizes different supercapatteries based on different electrodes and electrolytes, their energy, and power density. At the negatrode, mostly activated carbon of different sources was used in asymmetric battery//EDLC and pseudocapacitive//EDLC type supercapatteries. On the other hand, different metal iodide (BiOI-Bi_9I_2)[57], metal oxides (β-$NiMoO_4$[58], Phosphate ion-functionalized NiO (P-NiO)[59], $Zn_{0.5}CoO_{0.5}Mn(PO_4)_2$[60], $Co_3(PO_4)_2$)[61], $Co_{0.5}Ni_{0.5}WO_4$[62], etc.), metal hydroxides (Co–Ni LDH [63]), metal sulfides ($FeCoCuS_2$[64], $Co_{0.125}Cu_{0.375}Mn_{0.500}S$ [65], etc.), composites (Co-MOF-PAN [66]I, Sr_3P_2-PANI [67], MWCNT-$NiMnPO_4$[68], graphitic carbon nitride (g-C_3N_4)-$BiVO_4$[69], Zn-Carbon cloths,[70], etc.), etc. were used for positrode.

Preprints (www.preprints.org) | NOT PEER-REVIEWED | Posted: 6 December 2023 doi:10.20944/preprints202312.0355.v1

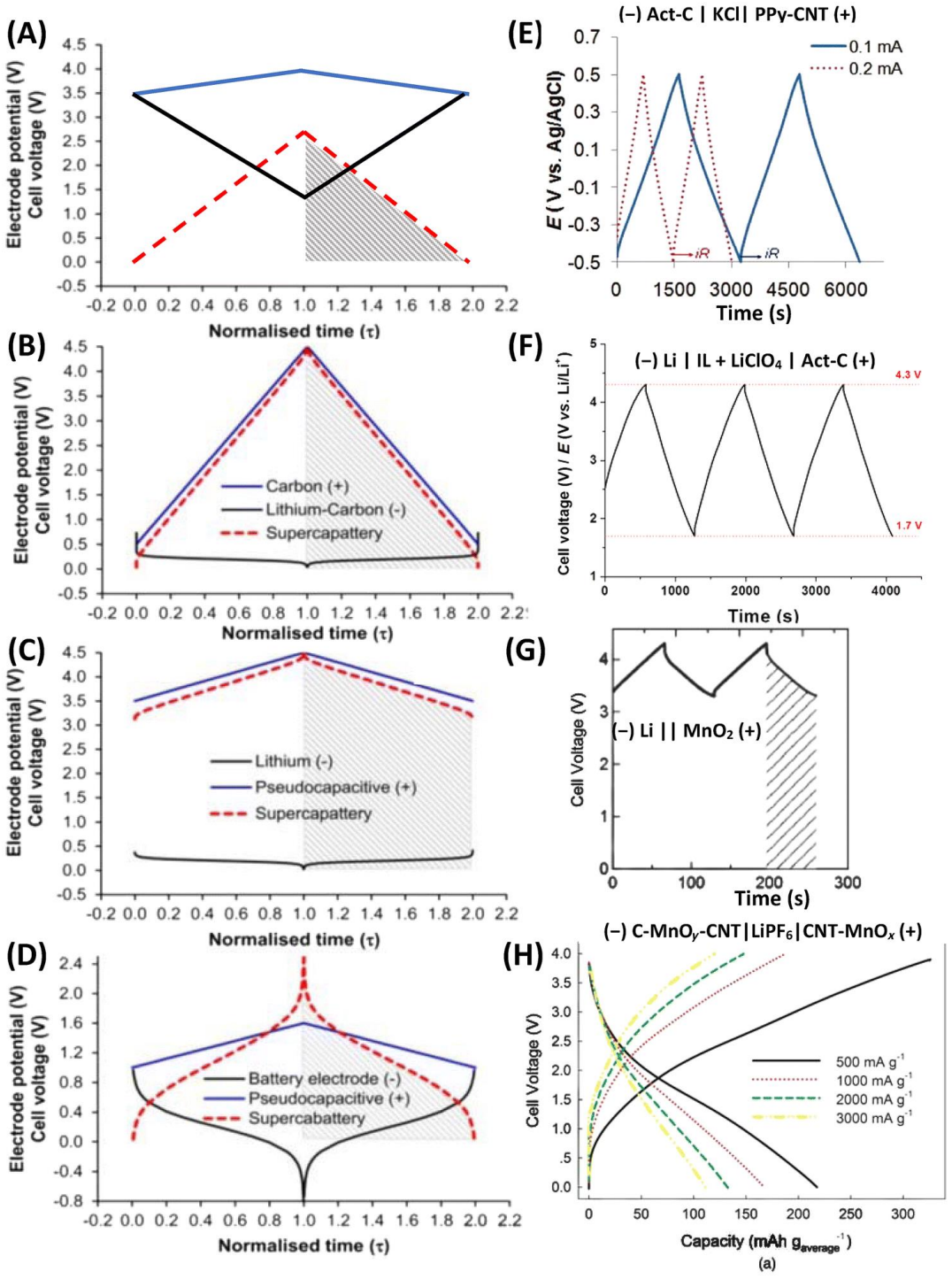

Figure 12. Calculated GCD plots of positrodes (blue lines), negatrodes (black lines) and relevant cells (red dash lines): a) hypothetical pseudocapacitor with an Act-C negatrode and a pseudocapacitive positrode and a hypothetical supercapattery with a negatrode of Li metal or lithiated carbon and b) an Act-C positrode or c) a pseudocapacitive positrode. d**)** A hypothetical supercapattery with a typical battery-type negatrode and a pseudocapacitive positrode. e) Experimental demonstration of (a), (−) Act-C ׀ KCl ׀ PPy-CNT (+). f) Experimental demonstration of (b), (−) Li ׀ IL + $LiClO_4$ ׀ Act-C (+). g) Experimental demonstration of (c), (−) Li ׀ PEO-LiTFSI ׀ LTAP ׀ 1.0 M LiCl aq. ׀ MnO_2 (+). h) Experimental demonstration of (d), (−) C-MnO_y-CNT ׀ $LiPF_6$׀ MnOx-CNT (+) [14].

Preprints (www.preprints.org) | NOT PEER-REVIEWED | Posted: 6 December 2023 doi:10.20944/preprints202312.0355.v1

Table 2. Performance of supercapatteries with different configurations. The data was collected from articles published during the last four years (2020-2023).

Device configuration	Electrolyte	Electrode Type	Energy density (Wh/kg)	Power density (W/kg)	Publication Year	Reference
$CeNiO_3$/Ni foam (symmetric)	6M KOH	(+)RB//RB(-)	38.70 28.41	774.81 7750	2022	[72]
$CeNiO_3$/Ni foam (symmetric)	3M KOH	(+)RB//RB(-)	43.45	800	2022	[79]
BiOI-Bi_9I_2/Ni foam (symmetric)	6M KOH	(+)RB//RB(-)	38.2	2280.4	2020	[57]
β-$NiMoO_4$/Ni foam (symmetric)	3M KOH	(+)RB//RB(-)	35.8 21.3	981.56 19282.4	2020	[58]
Ni(py-TTF-py)(BPDC)/Ni foam//AC/NI foam	6M KOH	(+)RB//ED(-)	90.3 47.2	1180 10400	2023	[80]
AgSr-Phosphate/Ni foam//CNT/Ni foam	1M KOH	(+)RB//ED(-)	55.02 42.37	741.54 9075	2023	[81]
Mxene/Ni foam//AC/Ni foam	1M KOH	(+)RB//ED(-)	68.8	1120	2023	[82]
NiS/Ni foam//AC/Ni foam	1M KOH	(+)RB//ED(-)	61.76	1275	2023	[83]
Fe_2O_3-α-$Ni(OH)_2$/Ni foam//AC/Ni foam	1M KOH	(+)RB//ED(-)	44.51	2465	2023	[84]
CoMnS-rGO/Ni foam//AC/Ni foam	1M KOH	(+)RB//ED(-)	45.6	2880	2023	[85]
CoCuP/Ni foam//O, N, S-AC/Ni foam	6M KOH	(+)RB//ED(-)	37.3 18.4	915 12308.8	2023	[73]
Fe-Mg MOF/Ni foam//AC/Ni foam	KOH	(+)RB//ED(-)	57	2393	2023	[86]
$Ag_2Co_3(PO6)_2$/Ni foam//CNT/Ni foam	1M KOH	(+)RB//ED(-)	40.92 33.26	1237.5 4125	2022	[87]
SrS/Ni foam//AC/Ni foam	KOH	(+)RB//ED(-)	44.39 12.9	595 8400	2022	[88]
CeO_2-ZnO-$ZnWO_4$-AC/Ni foam//AC/Ni foam	2M KOH	(+)RB//ED(-)	56.92	2000	2022	[89]
MnS/Ni foam//AC/Ni foam	KOH	(+)RB//ED(-)	127.5	2550	2022	[90]
WS/Ni foam//AC/Ni foam	1M KOH	(+)RB//ED(-)	45.2	608	2022	[91]
NiCo LDH/Ni foam//AC/Ni foam	6M KOH	(+)RB//ED(-)	20.5 9.01	774.5 8522.7	2022	[63]
$NiCo_2S_4$-graphene/Ni foam//AC-graphene/Ni foam	4M KOH + carboxymethyl cellulose	(+)RB//ED(-)	80	4000	2022	[92]
$LaMnO_3$/carbon cloth//rGO/carbon cloth	1M KOH	(+)RB//ED(-)	154 72	324 14700	2022	[70]
$LaMnO_3$/carbon cloth//rGO/carbon cloth	1M $NaClO_4$	(+)RB//ED(-)	236	3630	2022	[70]
$LaMnO_3$/carbon cloth//rGO/carbon cloth	2M $LiPF_6$	(+)RB//ED(-)	123	1430	2022	[70]
NiFe-Phosphate/Ni foam//AC/Ni foam	1M KOH	(+)RB//ED(-)	45.6	2250	2022	[93]
2D MoO_3-S_4-C/Ni foam//rGO/Ni foam	6M KOH	(+)RB//ED(-)	129.6	11600	2021	[71]
Cu-MOF-PANI-rGO-Ag/Ni foam//AC/Ni foam	1M KOH	(+)RB//ED(-)	52 27.2	1192 10200	2021	[94]

 doi:10.20944/preprints202312.0355.v1

$Co_{0.5}Mn_{0.5}S$/Ni foam//AC/Ni foam	1M KOH	(+)RB//E D(-)	61.34 9.92	850 8500	2021	[95]
VSB-5-rGO/Ni foam//AC/Ni foam	1M NaOH	(+)RB//E D(-)	80.5	2216.5	2021	[96]
$FeCoCuS_2$/Ni foam//AC/Ni foam	3M KOH	(+)RB//E D(-)	48.2 27.2	820.1 25700.2	2021	[64]
$Co_{0.125}Cu_{0.375}Mn_{0.500}S$/Ni foam//AC/Ni foam	1M KOH	(+)RB//E D(-)	88.71 20	320 8000	2021	[65]
$Co_3(PO_4)_2$/Cu/Ni foam//AC/Ni foam	1M KOH	(+)RB//E D(-)	62.6 11.8	425 7924	2021	[97]
$NiMn(PO_4)_2$-PANI/Ni foam//AC/Ni foam	1M KOH	(+)RB//E D(-)	71.3	340	2021	[98]
$Co_3(PO_4)_2$/Ni foam//AC/Ni foam	1M KOH	(+)RB//E D(-)	34.8 10.0	425 6800	2021	[99]
$MnCo_2S_4$-Mxene/Ni foam//AC/Ni foam	3M KOH	(+)RB//E D(-)	25.6 12.44	400 6400	2021	[100]
$Co_3(PO_4)_2$/Ag/Ni foam//AC/Ni foam	1M KOH	(+)RB//E D(-)	65.8	510	2021	[101]
$Ni_{0.75}Mn_{0.25}(PO_4)_2$/Ni foam//AC/Ni foam	1M KOH	(+)RB//E D(-)	64.2	340	2021	[102]
$Co_{0.125}Cu_{0.375}Mn_{0.500}(PO_4)_2$/Ni foam//AC/Ni foam	1M KOH	(+)RB//E D(-)	56 16.88	800 6420	2021	[103]
Trypan blue-Ni-MOF/Ni foam//Azure A-graphene aerogel/Ni foam	3M KOH	(+)RB//E D(-)	66.55 11.11	349 4450	2021	[104]
NiO@$CuCo_2O_4$/MoNi/Ni foam//AC/Ni foam	2M KOH	(+)RB//E D(-)	80.6 63.8	692.8 14000	2021	[105]
$Zn_{0.5}Co_{0.5}S$/Ni foam//AC/Ni foam	2M KOH	(+)RB//E D(-)	49 23	957 9413	2021	[106]
$Co_{0.5}Cu_{0.5}Mn(PO_4)_2$/Ni foam//AC/Ni foam	1M KOH	(+)RB//E D(-)	55 19	800 6400	2021	[107]
Ni-Co-Bi double hydroxide/Ni-Co-B/Ni foam//AC/Ni foam	2M KOH	(+)RB//E D(-)	62.8	800	2020	[108]
Phosphate ion-functionalized NiO (P-NiO)/Ni foam//AC/Ni foam	3M KOH	(+)RB//E D(-)	53.4 24.7	800 12000	2020	[59]
Sr_3P_2-PANI/Ni foam//AC/Ni foam	1M KOH	(+)RB//E D(-)	28.9 10.95	1020 5100	2020	[67]
$Zn_{0.5}CoO_{0.5}Mn(PO_4)_2$/Ni foam//AC/Ni foam	1M KOH	(+)RB//E D(-)	45.45 6.86	425 4250	2020	[60]
$Co_3(PO_4)_2$/Ni-Co-O/Ni foam//Fe_2P/graphene hydrogel/Ni foam	PVA-KOH	(+)RB//E D(-)	95 18	400 4000	2020	[61]
$Co_{0.5}Ni_{0.5}WO_4$/Ni foam//AC/Ni foam	2M KOH	(+)RB//E D(-)	42.2	1047.7	2020	[62]
Co-MOF-PANI/Ni foam//AC/Ni foam	1M KOH	(+)RB//E D(-)	23.11 8.906	1600 6400	2020	[66]
WO_3-WS_2-MWCNT/Ni foam//AC/Ni foam	3M KOH	(+)PC//E D(-)	86 24	848 11828	2023	[109]
Ni-Co-Mg MOF/MoS_2/Ni foam//AC/Ni foam	1M KOH	(+)PC//E D(-)	107.32	1350	2023	[110]
NH_4MnPO_4@Graphene QD/Graphite//rGO/Graphite	3M H_2SO_4 3M H_2SO_4 + 0.025M (KI/$VOSO_4$)	(+)PC//E D(-)	199 311	450 450	2022	[76]
$Ni_3(PO_4)_2$-MWCNTs/Ni foam//AC/Ni foam		(+)PC//E D(-)	94.4 24.82	340 10200	2022	[111]
Mn-V-Sn oxyhydroxide/Ni foam//N-carbon/Ni foam	1M KOH	(+)PC//E D(-)	70.6 17.1	1372.4 18861.3	2022	[112]

Preprints (www.preprints.org) | NOT PEER-REVIEWED | Posted: 6 December 2023 doi:10.20944/preprints202312.0355.v1

NH_4OH-ZIF/Ni foam//GO/Ni foam	6M KOH	(+)PC//ED(-)	4.16	20000	2022	[113]
CoS-$Co_3(PO_4)_2$/Ni foam//AC/Ni foam	1M KOH	(+)PC//ED(-)	34.68 63.93	13600 850	2021	[114]
Fe_3O_4@N-carbon-rGO/Ni foam//rGO/Ni foam	6M KOH	(+)PC//ED(-)	46 10	750 7500	2021	[115]
MWCNT-$NiMnPO_4$/Ni foam//AC/Ni foam	2M KOH	(+)PC//ED(-)	698 43	78 5780	2020	[68]
P-NiCoB/Ni foam//rGO/Ni foam	2M KOH	(+)RB//PC(-)	63.125 41.56	750 15000	2023	[74]
$CoMn_2O_4$/N-graphene/Ni foam//N-graphene/Ni foam	PVA-KOH	(+)RB//PC(-)	44.1 20.3	992.6 12430	2021	[116]
graphitic carbon nitride (g-C_3N_4)-$BiVO_4$/Graphite paper (symmetric)	3.5M KOH	(+)PC//PC(-)	61 7.2	1996 16200	2020	[69]
Zn-Carbon cloths//S/P doped carbon (S/p-C)/graphite rod	0.5M K_2SO_4 1M KBr	(+)PC//PC(-)	270 181	185 9300	2020	[75]

ED → electrical double layer capacitive type; PC → pseudocapacitive type; RB → rechargeable battery type.

In the electrolyte, mostly, aqueous KOH of different concentrations has been used in supercapatteries [57,71–74]. Other electrolytes used are $LiPF_6$[70], K_2SO_4[75], H_2SO_4[76], KBr [75], $NaClO_4$[70], PVA-KOH [61], KI/$VOSO_4$[76], etc. Electrolytes with additional redox species have been investigated in supercapatteries with significantly enhanced energy capacity [27,53,77]. Also, EDLC materials with redox electrolytes showed enhanced performance [78].

3.3.2. Performance and Experimental Evaluation of Supercapatteries

Figure 13 shows Ragone plots of supercapatteries reported in published articles during the last four years, from 2020 to 2023. The corresponding data is summarized in Table 2. Primarily, the reported supercapatteries performed either like an EDLC or an RB. However, Devi et al. reported a Na-ion supercapattery with outstanding specific energy of 236 W h kg^{-1} at a higher specific power of 3630 W kg^{-1} with appreciable retention of over 95% even at the 10,000th cycle [70]. It is important to note that capacitance can be used only when there is a linear relationship between charge and voltage, and the capacitance value should be a single constant value in the chosen potential window; any deviation from this behavior requires that integration be used to calculate the charge being stored or delivered. Also, capacity instead of capacitance should be measured for RBs. As Chen pointed out, many authors have ignored the critical differences between SCs and RBs as they applied the concept of pseudocapacitance to some new battery-type materials [17]. As a result, deceptively high specific capacitance values have been claimed, and the high specific capacitance was also used in calculating specific energy.

Preprints (www.preprints.org) | NOT PEER-REVIEWED | Posted: 6 December 2023 doi:10.20944/preprints202312.0355.v1

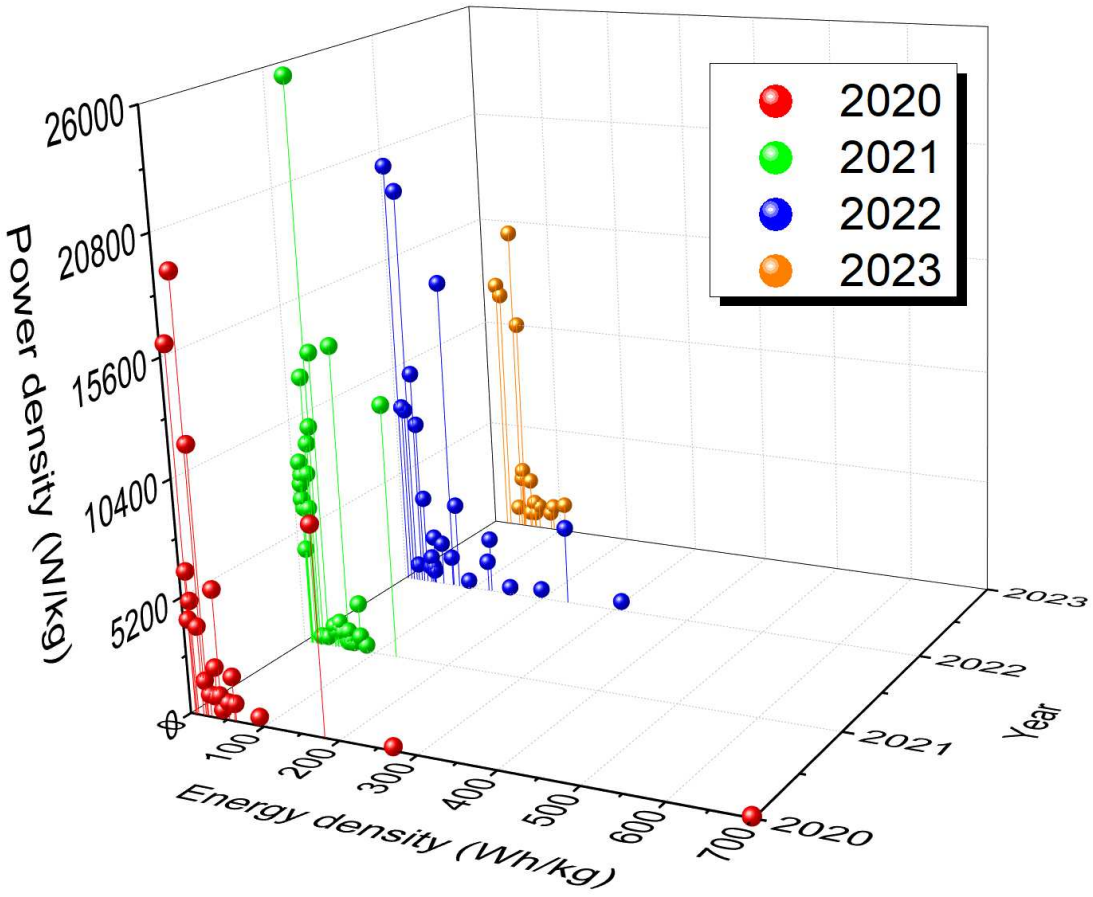

Figure 13. Ragone plots of different supercapatteries reported over the last four years (20020-2023) showing relative energy and power density.

3.4. Classification of EES Devices

From the above discussion, it is evident that RBs and SCs belong to EES, as shown in Figure 14, where EDLCs and PCs belong to SCs. However, placing HSCs and supercapatteries in the classification tree is inconsistent throughout the literature [8,11,17,19,26–28]. Even ASCs were placed parallel to HSCs or in place of HSCs, making HSCs a subclass of ASCs [19]. Initially, HSCs appeared to be defined as hybrids of EDLCs and PCs, whereas supercapatteries were considered as hybrids of EDLCs and RBs. Guan et al. proposed defining and differentiating storage mechanisms in EES devices according to Figure 9 without explicitly differentiating ASCs and HSCs [18]. Considering all possible combinations of electrode materials and storage mechanisms, EES devices were classified vividly in a tabulated form (Table 1)[17], where the combination results in nine different devices depending on electrode materials and storage mechanisms.

Preprints (www.preprints.org) | NOT PEER-REVIEWED | Posted: 6 December 2023 doi:10.20944/preprints202312.0355.v1

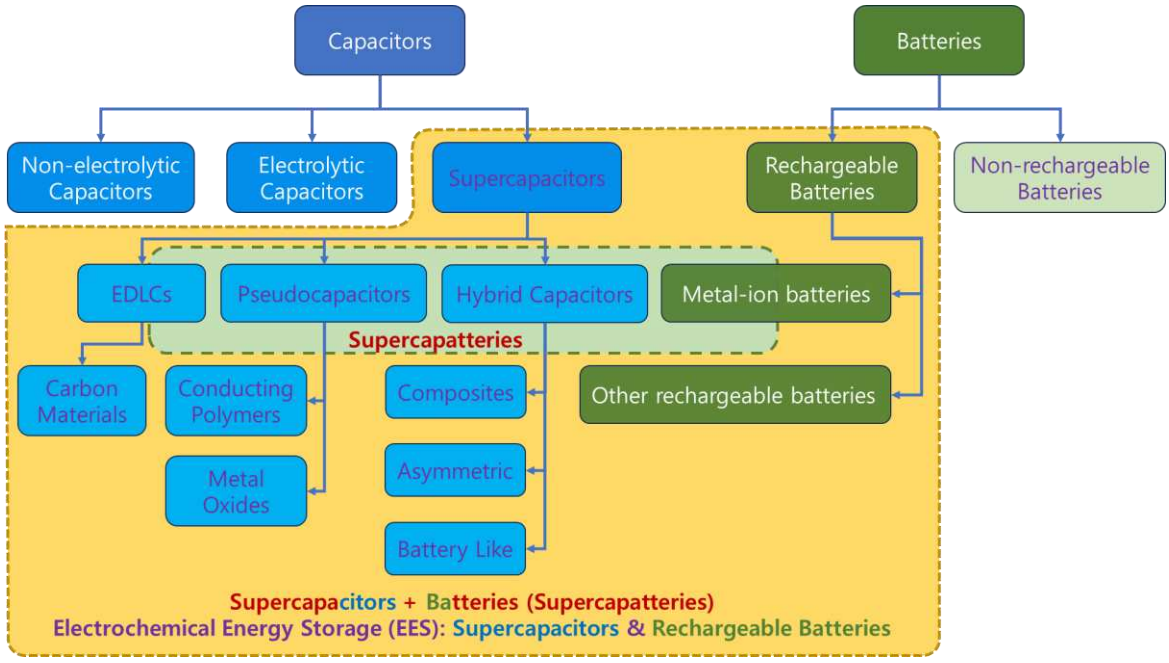

Figure 14. Classification of various electrochemical energy storage (EES) systems based on storage mechanisms [8]. EES and supercapatteries are highlighted in yellow and green rectangles bordered with dashed lines [42].

4. Summary and perspective

All supercapatteries are hybrid EES devices, but not all hybrid EES devices are supercapatteries. Supercapatteries are envisioned as a technology that will mutually complement the drawbacks of RBs and SCs. Supercapatteries are EES devices that can integrate the benefits of RBs and SCs using all three charge storage mechanisms: non-Faradaic capacitive storage (EDL capacitive storage), capacitive Faradaic storage (pseudocapacitive storage) and non-capacitive Faradaic storage (rechargeable battery-type storage or Nernstian charge storage). Moreover, supercapatteries can be made of EDLCs, non-faradaic capacitive, using a redox electrolyte. In summary, supercapatteries have gained increasing attention in the EES field, as seen in the growing number of publications using the term "supercapattery". The development of supercapattery materials can benefit from the advances in battery and supercapacitor materials. Nanotechnologies and engineering will play a more significant role in advancing micro supercapatteries in powering IoTs. Like LiBs, supercapatteries are on the verge of revolutionizing the whole ecosystem of energy storage and related industries, including renewable energy, portable electronics, and the EV industry.

Conflicts of Interest: The authors declare that there is no conflict of interest regarding the publication of this paper.

Acknowledgments: This work was supported by the Brain Pool Program through the National Research Foundation of Korea (NRF) funded by the Ministry of Science and ICT (RS-2023-00222798 and RS-2022-00156291).

References

1. A.J. Gabric, The Climate Change Crisis: A Review of Its Causes and Possible Responses, Atmosphere (Basel). 14 (2023) 1081. https://doi.org/10.3390/atmos14071081.
2. K. Abbass, M.Z. Qasim, H. Song, M. Murshed, H. Mahmood, I. Younis, A review of the global climate change impacts, adaptation, and sustainable mitigation measures, Environmental Science and Pollution Research. 29 (2022) 42539–42559. https://doi.org/10.1007/s11356-022-19718-6.

3. A. Dutta, S. Mitra, M. Basak, T. Banerjee, A comprehensive review on batteries and supercapacitors: Development and challenges since their inception, Energy Storage. 5 (2023). https://doi.org/10.1002/est2.339.
4. J.B. Goodenough, K.-S. Park, The Li-Ion Rechargeable Battery: A Perspective, J Am Chem Soc. 135 (2013) 1167–1176. https://doi.org/10.1021/ja3091438.
5. H.S. Choi, C.R. Park, Theoretical guidelines to designing high performance energy storage device based on hybridization of lithium-ion battery and supercapacitor, J Power Sources. 259 (2014) 1–14. https://doi.org/10.1016/j.jpowsour.2014.02.001.
6. M.S. Kiai, O. Eroglu, N. Aslfattahi, Metal-Ion Batteries: Achievements, Challenges, and Prospects, Crystals (Basel). 13 (2023). https://doi.org/10.3390/cryst13071002.
7. J. Verma, D. Kumar, Metal-ion batteries for electric vehicles: current state of the technology, issues and future perspectives, Nanoscale Adv. 3 (2021) 3384–3394. https://doi.org/10.1039/d1na00214g.
8. D.P. Chatterjee, A.K. Nandi, A review on the recent advances in hybrid supercapacitors, J Mater Chem A Mater. 9 (2021) 15880–15918. https://doi.org/10.1039/d1ta02505h.
9. D. Gao, Z. Luo, C. Liu, S. Fan, A survey of hybrid energy devices based on supercapacitors, Green Energy and Environment. 8 (2023) 972–988. https://doi.org/10.1016/j.gee.2022.02.002.
10. A. Yu, V. Chabot, J. Zhang, ELECTROCHEMICAL SUPERCAPACITORS FOR ENERGY STORAGE AND DELIVERY FUNDAMENTALS AND APPLICATIONS, 2013.
11. M.Z. Iqbal, M.M. Faisal, S.R. Ali, Integration of supercapacitors and batteries towards high-performance hybrid energy storage devices, Int J Energy Res. 45 (2021) 1449–1479. https://doi.org/10.1002/er.5954.
12. L. Xia, B. Tang, J. Wei, Z. Zhou, Recent Advances in Alkali Metal-Ion Hybrid Supercapacitors, Batter Supercaps. 4 (2021) 1108–1121. https://doi.org/10.1002/batt.202000332.
13. D. Majumdar, M. Mandal, S.K. Bhattacharya, Journey from supercapacitors to supercapatteries: recent advancements in electrochemical energy storage systems, Emergent Mater. 3 (2020) 347–367. https://doi.org/10.1007/s42247-020-00090-5.
14. L. Yu, G.Z. Chen, Supercapatteries as High-Performance Electrochemical Energy Storage Devices, Electrochemical Energy Reviews. 3 (2020) 271–285. https://doi.org/10.1007/s41918-020-00063-6.
15. M. Prajapati, V. Singh, M. V. Jacob, C. Ravi Kant, Recent advancement in metal-organic frameworks and composites for high-performance supercapatteries, Renewable and Sustainable Energy Reviews. 183 (2023). https://doi.org/10.1016/j.rser.2023.113509.
16. A.J. Bard, L.R. Faulkner, H.S. White, Electrochemical methods: fundamentals and applications, John Wiley & Sons, 2022.
17. G.Z. Chen, Supercapacitor and supercapattery as emerging electrochemical energy stores, International Materials Reviews. 62 (2017) 173–202. https://doi.org/10.1080/09506608.2016.1240914.
18. L. Guan, L. Yu, G.Z. Chen, Capacitive and non-capacitive faradaic charge storage, Electrochim Acta. 206 (2016) 464–478. https://doi.org/10.1016/j.electacta.2016.01.213.
19. Y. Shao, M.F. El-Kady, J. Sun, Y. Li, Q. Zhang, M. Zhu, H. Wang, B. Dunn, R.B. Kaner, Design and Mechanisms of Asymmetric Supercapacitors, Chem Rev. 118 (2018) 9233–9280. https://doi.org/10.1021/acs.chemrev.8b00252.
20. S. Sarker, H.W. Seo, Y.-K. Jin, K.-S. Lee, M. Lee, D.M. Kim, On the Hysteresis of Current Density-Voltage Curves of Dye-sensitized Solar Cells, Electrochim Acta. 182 (2015) 493–499. https://doi.org/10.1016/j.electacta.2015.09.083.
21. S. Sarker, A.J.S. Ahammad, H.W. Seo, D.M. Kim, Electrochemical Impedance Spectra of Dye-Sensitized Solar Cells: Fundamentals and Spreadsheet Calculation, International Journal of Photoenergy. 2014 (2014) 1–17. https://doi.org/10.1155/2014/851705.
22. M. ITAGAKI, S. SUZUKI, I. SHITANDA, K. WATANABE, Electrochemical Impedance and Complex Capacitance to Interpret Electrochemical Capacitor, Electrochemistry. 75 (2007) 649–655. https://doi.org/10.5796/electrochemistry.75.649.
23. T.S. Mathis, N. Kurra, X. Wang, D. Pinto, P. Simon, Y. Gogotsi, Energy Storage Data Reporting in Perspective—Guidelines for Interpreting the Performance of Electrochemical Energy Storage Systems, Adv Energy Mater. 9 (2019). https://doi.org/10.1002/aenm.201902007.
24. K. Kannadasan, V. Sankar Devi, S. Archana, P. Thomas, P. Elumalai, Deconvolution of capacitive and diffusive charge/lithium storage in lyophilized NiCo2S4-NiCo2O4 composite for supercapattery and lithium-ion battery, New Journal of Chemistry. 47 (2023) 13963–13978. https://doi.org/10.1039/d3nj01663c.

25. M. Winter, R.J. Brodd, What Are Batteries, Fuel Cells, and Supercapacitors?, Chem Rev. 104 (2004) 4245–4270. https://doi.org/10.1021/cr020730k.
26. L. Yu, G.Z. Chen, Redox electrode materials for supercapatteries, J Power Sources. 326 (2016) 604–612. https://doi.org/10.1016/j.jpowsour.2016.04.095.
27. B. Akinwolemiwa, G.Z. Chen, Fundamental consideration for electrochemical engineering of supercapattery, J Braz Chem Soc. 29 (2018) 960–972. https://doi.org/10.21577/0103-5053.20180010.
28. S. Dsoke, K. Pfeifer, Z. Zhao, The role of nanomaterials for supercapacitors and hybrid devices, in: Frontiers of Nanoscience, Elsevier Ltd., 2021: pp. 99–136. https://doi.org/10.1016/B978-0-12-821434-3.00001-6.
29. B. Akinwolemiwa, C. Wei, G.Z. Chen, Mechanisms and Designs of Asymmetrical Electrochemical Capacitors, Electrochim Acta. 247 (2017) 344–357. https://doi.org/10.1016/j.electacta.2017.06.088.
30. J. Zhao, A.F. Burke, Review on supercapacitors: Technologies and performance evaluation, Journal of Energy Chemistry. 59 (2021) 276–291. https://doi.org/10.1016/j.jechem.2020.11.013.
31. P. Sinha, K.K. Kar, Introduction to Supercapacitors, in: K.K. Kar (Ed.), Handbook of Nanocomposite Supercapacitor Materials II, Springer, 2020: pp. 1–28. https://doi.org/10.1007/978-3-030-52359-6_1.
32. M.Z. Iqbal, U. Aziz, Supercapattery: Merging of battery-supercapacitor electrodes for hybrid energy storage devices, J Energy Storage. 46 (2022). https://doi.org/10.1016/j.est.2021.103823.
33. Poonam, K. Sharma, A. Arora, S.K. Tripathi, Review of supercapacitors: Materials and devices, J Energy Storage. 21 (2019) 801–825. https://doi.org/10.1016/j.est.2019.01.010.
34. V. Augustyn, P. Simon, B. Dunn, Pseudocapacitive oxide materials for high-rate electrochemical energy storage, Energy Environ Sci. 7 (2014) 1597. https://doi.org/10.1039/c3ee44164d.
35. Y. Liu, S.P. Jiang, Z. Shao, Intercalation pseudocapacitance in electrochemical energy storage: recent advances in fundamental understanding and materials development, Mater Today Adv. 7 (2020) 100072. https://doi.org/10.1016/j.mtadv.2020.100072.
36. Y. Jiang, J. Liu, Definitions of Pseudocapacitive Materials: A Brief Review, Energy and Environmental Materials. 2 (2019) 30–37. https://doi.org/10.1002/eem2.12028.
37. B.E. Conway, Two-dimensional and quasi-two-dimensional isotherms for Li intercalation and upd processes at surfaces, Electrochim Acta. 38 (1993) 1249–1258. https://doi.org/10.1016/0013-4686(93)80055-5.
38. E. Herrero, L.J. Buller, H.D. Abruña, Underpotential Deposition at Single Crystal Surfaces of Au, Pt, Ag and Other Materials, Chem Rev. 101 (2001) 1897–1930. https://doi.org/10.1021/cr9600363.
39. H.W. Park, K.C. Roh, Recent advances in and perspectives on pseudocapacitive materials for Supercapacitors–A review, J Power Sources. 557 (2023) 232558. https://doi.org/10.1016/j.jpowsour.2022.232558.
40. R. Barik, P.P. Ingole, Challenges and prospects of metal sulfide materials for supercapacitors, Curr Opin Electrochem. 21 (2020) 327–334. https://doi.org/10.1016/j.coelec.2020.03.022.
41. T. Brousse, D. Bélanger, J.W. Long, To Be or Not To Be Pseudocapacitive?, J Electrochem Soc. 162 (2015) A5185–A5189. https://doi.org/10.1149/2.0201505jes.
42. P. Lamba, P. Singh, P. Singh, P. Singh, Bharti, A. Kumar, M. Gupta, Y. Kumar, Recent advancements in supercapacitors based on different electrode materials: Classifications, synthesis methods and comparative performance, J Energy Storage. 48 (2022). https://doi.org/10.1016/j.est.2021.103871.
43. A.G. Olabi, Q. Abbas, P.A. Shinde, M.A. Abdelkareem, Rechargeable batteries: Technological advancement, challenges, current and emerging applications, Energy. 266 (2023) 126408. https://doi.org/10.1016/j.energy.2022.126408.
44. S.A. Khan, S. Ali, K. Saeed, M. Usman, I. Khan, Advanced cathode materials and efficient electrolytes for rechargeable batteries: Practical challenges and future perspectives, J Mater Chem A Mater. 7 (2019) 10159–10173. https://doi.org/10.1039/c9ta00581a.
45. Q. Liu, H. Wang, C. Jiang, Y. Tang, Multi-ion strategies towards emerging rechargeable batteries with high performance, Energy Storage Mater. 23 (2019) 566–586. https://doi.org/10.1016/j.ensm.2019.03.028.
46. B. Halford, Lithium-ion battery pioneers nab 2019 Nobel Prize in Chemistry, (2019). https://cen.acs.org/people/nobel-prize/Li-ion-batteries-win-2019-Nobel-Prize-in-Chemistry/97/web/2019/10 (accessed November 25, 2023).
47. W. Chen, J. Liang, Z. Yang, G. Li, A Review of Lithium-Ion Battery for Electric Vehicle Applications and Beyond, Energy Procedia. 158 (2019) 4363–4368. https://doi.org/10.1016/j.egypro.2019.01.783.

48. P.U. Nzereogu, A.D. Omah, F.I. Ezema, E.I. Iwuoha, A.C. Nwanya, Anode materials for lithium-ion batteries: A review, Applied Surface Science Advances. 9 (2022) 100233. https://doi.org/10.1016/j.apsadv.2022.100233.
49. S.-W. WOO, K. DOKKO, H. NAKANO, K. KANAMURA, Bimodal Porous Carbon as a Negative Electrode Material for Lithium-Ion Capacitors, Electrochemistry. 75 (2007) 635–640. https://doi.org/10.5796/electrochemistry.75.635.
50. H. Wang, C. Zhu, D. Chao, Q. Yan, H.J. Fan, Nonaqueous Hybrid Lithium-Ion and Sodium-Ion Capacitors, Advanced Materials. 29 (2017). https://doi.org/10.1002/adma.201702093.
51. Z.-K. Chen, J.-W. Lang, L.-Y. Liu, L.-B. Kong, Preparation of a NbN/graphene nanocomposite by solution impregnation and its application in high-performance Li-ion hybrid capacitors, RSC Adv. 7 (2017) 19967–19975. https://doi.org/10.1039/C7RA01671A.
52. M. Arnaiz, J.L. Gómez-Cámer, J. Ajuria, F. Bonilla, B. Acebedo, M. Jáuregui, E. Goikolea, M. Galceran, T. Rojo, High Performance Titanium Antimonide $TiSb_2$ Alloy for Na-Ion Batteries and Capacitors, Chemistry of Materials. 30 (2018) 8155–8163. https://doi.org/10.1021/acs.chemmater.8b02639.
53. B. Akinwolemiwa, C. Peng, G.Z. Chen, Redox Electrolytes in Supercapacitors, J Electrochem Soc. 162 (2015) A5054–A5059. https://doi.org/10.1149/2.0111505jes.
54. W. Shimizu, S. Makino, K. Takahashi, N. Imanishi, W. Sugimoto, Development of a 4.2 V aqueous hybrid electrochemical capacitor based on MnO2 positive and protected Li negative electrodes, J Power Sources. 241 (2013) 572–577. https://doi.org/10.1016/j.jpowsour.2013.05.003.
55. S. Makino, Y. Shinohara, T. Ban, W. Shimizu, K. Takahashi, N. Imanishi, W. Sugimoto, 4 V class aqueous hybrid electrochemical capacitor with battery-like capacity, RSC Adv. 2 (2012) 12144. https://doi.org/10.1039/c2ra22265e.
56. D. Hu, C. Peng, G.Z. Chen, Electrodeposition of Nonconducting Polymers: Roles of Carbon Nanotubes in the Process and Products, ACS Nano. 4 (2010) 4274–4282. https://doi.org/10.1021/nn100849d.
57. S. Park, N.M. Shinde, P. V. Shinde, D. Lee, J.M. Yun, K.H. Kim, Chemically grown bismuth-oxy-iodide (BiOI/Bi9I2) nanostructure for high performance battery-type supercapacitor electrodes, Dalton Transactions. 49 (2020) 774–780. https://doi.org/10.1039/c9dt04365a.
58. N. Padmanathan, H. Shao, K.M. Razeeb, Honeycomb micro/nano-architecture of stable β-NiMoO4 electrode/catalyst for sustainable energy storage and conversion devices, Int J Hydrogen Energy. 45 (2020) 30911–30923. https://doi.org/10.1016/j.ijhydene.2020.08.058.
59. M. Kang, H. Zhou, B. Qin, N. Zhao, B. Lv, Ultrathin nanosheet-assembled, phosphate ion-functionalized NiO microspheres as efficient supercapacitor materials, ACS Appl Energy Mater. 3 (2020) 9980–9988. https://doi.org/10.1021/acsaem.0c01653.
60. M.Z. Iqbal, J. Khan, H.T.A. Awan, M. Alzaid, A.M. Afzal, S. Aftab, Cobalt-manganese-zinc ternary phosphate for high performance supercapattery devices, Dalton Transactions. 49 (2020) 16715–16727. https://doi.org/10.1039/d0dt03313h.
61. T. Yan, H. Feng, X. Ma, L. Han, L. Zhang, S. Cao, Regulating the electrochemical behaviours of a hierarchically structured Co3(PO4)2/Ni-Co-O for a high-performance all-solid-state supercapacitor, Dalton Transactions. 49 (2020) 10621–10630. https://doi.org/10.1039/d0dt01818j.
62. B. Huang, H. Wang, S. Liang, H. Qin, Y. Li, Z. Luo, C. Zhao, L. Xie, L. Chen, Two-dimensional porous cobalt–nickel tungstate thin sheets for high performance supercapattery, Energy Storage Mater. 32 (2020) 105–114. https://doi.org/10.1016/j.ensm.2020.07.014.
63. P. Thondaiman, C.J. Raj, R. Velayutham, A.D. Savariraj, R. Manikandan, V. Cristobal, B.C. Kim, Engineering redox active sites enriched 3D-on-2D bimetallic double layered hydroxide electrode for supercapatteries, Mater Today Energy. 30 (2022). https://doi.org/10.1016/j.mtener.2022.101182.
64. M. Amiri, S.E. Moosavifard, S.S. Hosseiny Davarani, M. Shamsipur, Novel Rugby-Ball-like FeCoCuS2Triple-Shelled Hollow Nanostructures with Enhanced Performance for Supercapattery, Energy and Fuels. 35 (2021) 15108–15117. https://doi.org/10.1021/acs.energyfuels.1c01807.
65. M. Alzaid, M.Z. Iqbal, J. Khan, S. Alam, N.M.A. Hadia, W.S. Mohamed, Drive towards Sonochemically Synthesized Ternary Metal Sulfide for High-Energy Supercapattery, Energy Technology. 9 (2021). https://doi.org/10.1002/ente.202100110.
66. M.Z. Iqbal, M.M. Faisal, S.R.A. Meshal Alzaid, A facile approach to investigate the charge storage mechanism of MOF/PANI based supercapattery devices, Solid State Ion. 354 (2020). https://doi.org/10.1016/j.ssi.2020.115411.

67. M.Z. Iqbal, M.M. Faisal, S.R. Ali, A.M. Afzal, M.R. Abdul Karim, M.A. Kamran, T. Alharbi, Strontium phosphide-polyaniline composites for high performance supercapattery devices, Ceram Int. 46 (2020) 10203–10214. https://doi.org/10.1016/j.ceramint.2020.01.012.
68. V. Sharmila, R. Packiaraj, N. Nallamuthu, M. Parthibavarman, Fabrication of MWCNTs wrapped nickel manganese phosphate asymmetric capacitor as a supercapattery electrode for energy storage applications, Inorg Chem Commun. 121 (2020). https://doi.org/10.1016/j.inoche.2020.108194.
69. C. Murugan, K. Subramani, R. Subash, M. Sathish, A. Pandikumar, High-performance high-voltage symmetric supercapattery based on a graphitic carbon nitride/bismuth vanadate nanocomposite, Energy and Fuels. 34 (2020) 16858–16869. https://doi.org/10.1021/acs.energyfuels.0c03261.
70. V. Sankar Devi, K. Kannadasan, P.C. Sharafudeen, P. Elumalai, Performance of sodium-ion supercapattery using LaMnO3 and rGO in non-aqueous electrolyte, New Journal of Chemistry. 46 (2022) 15130–15144. https://doi.org/10.1039/d2nj01898e.
71. L. Gurusamy, L. Karuppasamy, S. Anandan, N. Liu, G.J. Lee, C.H. Liu, J.J. Wu, Enhanced performance of charge storage supercapattery by dominant oxygen deficiency in crystal defects of 2-D MoO3-x nanoplates, Appl Surf Sci. 541 (2021). https://doi.org/10.1016/j.apsusc.2020.148676.
72. M.P. Harikrishnan, A. Chandra Bose, Binder-free synthesis of cerium nickel oxide for supercapattery devices, Int J Energy Res. 46 (2022) 21826–21840. https://doi.org/10.1002/er.8728.
73. A.M. Kale, R. Velayutham, A.D. Savariraj, M. Demir, B.C. Kim, Unravelling the influence of interfacial tailoring in metal-organic framework-derived ultrathin sheets of Co2P/Cu3P for high-performance hybrid supercapacitor, Materials Today Sustainability. 21 (2023). https://doi.org/10.1016/j.mtsust.2023.100335.
74. A.T. Sivagurunathan, T. Kavinkumar, S. Seenivasan, Y. Kwon, D.-H. Kim, Enhancing high-performance supercapattery electrodes: harnessing structural and compositional synergies via phosphorus doping on bimetallic boride for rapid charging , J Mater Chem A Mater. (2023). https://doi.org/10.1039/d3ta04124g.
75. F. Yu, C. Zhang, F. Wang, Y. Gu, P. Zhang, E.R. Waclawik, A. Du, K. Ostrikov, H. Wang, A zinc bromine "supercapattery" system combining triple functions of capacitive, pseudocapacitive and battery-type charge storage, Mater Horiz. 7 (2020) 495–503. https://doi.org/10.1039/c9mh01353a.
76. T.A. Raja, P. Vickraman, Role of dual redox additives KI/VOSO4 in manganese ammonium phosphate at graphene quantum dots for supercapattery, Int J Energy Res. 46 (2022) 9097–9113. https://doi.org/10.1002/er.7787.
77. J. Lee, P. Srimuk, S. Fleischmann, X. Su, T.A. Hatton, V. Presser, Redox-electrolytes for non-flow electrochemical energy storage: A critical review and best practice, Prog Mater Sci. 101 (2019) 46–89. https://doi.org/10.1016/j.pmatsci.2018.10.005.
78. B. Akinwolemiwa, C. Wei, Q. Yang, L. Yu, L. Xia, D. Hu, C. Peng, G.Z. Chen, Optimal Utilization of Combined Double Layer and Nernstian Charging of Activated Carbon Electrodes in Aqueous Halide Supercapattery through Capacitance Unequalization, J Electrochem Soc. 165 (2018) A4067–A4076. https://doi.org/10.1149/2.0031902jes.
79. M.P. Harikrishnan, A.C. Bose, Porous CeNiO3 with an enhanced electrochemical performance and prolonged cycle life (>50 000 cycles) via a lemon-assisted sol-gel autocombustion method, New Journal of Chemistry. 46 (2022) 15118–15129. https://doi.org/10.1039/d2nj02295h.
80. Z.H. Ren, Z.R. Zhang, L.J. Ma, C.Y. Luo, J. Dai, Q.Y. Zhu, Oxidatively Doped Tetrathiafulvalene-Based Metal-Organic Frameworks for High Specific Energy of Supercapatteries, ACS Appl Mater Interfaces. 15 (2023) 6621–6630. https://doi.org/10.1021/acsami.2c17523.
81. S.R. Ali, M.M. Faisal, S.L. Loredo, S.K. Gadi, K.C. Sanal, Anomalous electrochemical performance of binary silver–strontium phosphate-based electrode material in supercapattery, Ceram Int. 49 (2023) 18311–18321. https://doi.org/10.1016/j.ceramint.2023.02.203.
82. H.H. Hegazy, A.M. Afzal, E.R. Shaaban, M. Waqas Iqbal, S. Muhammad, A.A. Alahmari, Synthesis of MXene and design the high-performance energy harvesting devices with multifunctional applications, Ceram Int. 49 (2023) 1710–1719. https://doi.org/10.1016/j.ceramint.2022.09.135.
83. M.Z. Iqbal, U. Aziz, N. Amjad, S. Aftab, S.M. Wabaidur, Porous activated carbon and highly redox active transition metal sulfide by employing multi-synthesis approaches for battery-supercapacitor applications, Diam Relat Mater. 136 (2023). https://doi.org/10.1016/j.diamond.2023.110019.
84. S.K. Babu, B. Gunasekaran, Ultrathin α-Ni(OH)2 nanosheets coated on MOF-derived Fe2O3 nanorods as a potential electrode for solid-state hybrid supercapattery device, Electrochim Acta. 447 (2023). https://doi.org/10.1016/j.electacta.2023.142146.

85. M. Ali, A.M. Afzal, M.W. Iqbal, A. Ur Rehman, S.M. Wabaidur, E.A. Al-Ammar, S. Mumtaz, E.H. Choi, Synthesis and analysis of the impact of rGO on the structural and electrochemical performance of CoMnS for high-performance energy storage device, FlatChem. 40 (2023). https://doi.org/10.1016/j.flatc.2023.100518.
86. A. Zaka, M.W. Iqbal, A.M. Afzal, H. Hassan, H. Rafique, S.M. Wabaidur, A.M. Tawfeek, E. Elahi, A bimetallic Fe-Mg MOF with a dual role as an electrode in asymmetric supercapacitors and an efficient electrocatalyst for hydrogen evolution reaction (HER), RSC Adv. 13 (2023) 26528–26543. https://doi.org/10.1039/d3ra04279k.
87. S.R. Ali, M.M. Faisal, S. Pushpan, N.P. Aguilar, K.K. Singh, A. Cerdán-Pasarán, M.M.A. Rodríguez, E.M. Sánchez, A.T. Castro, S.L. Loredo, K.C. Sanal, Mesoporous silver-cobalt-phosphate nanostructures synthesized via hydrothermal and solid-state reaction for supercapattery devices, Int J Energy Res. 46 (2022) 23757–23774. https://doi.org/10.1002/er.8673.
88. M.Z. Iqbal, U. Aziz, M.W. Khan, S. Siddique, M. Alzaid, Strategies to enhance the electrochemical performance of strontium-based electrode materials for battery-supercapacitor applications, Journal of Electroanalytical Chemistry. 924 (2022). https://doi.org/10.1016/j.jelechem.2022.116868.
89. M.R. Khawar, N.A. Shad, S. Hussain, Y. Javed, M.M. Sajid, A. Jilani, M. Faheem, A. Asghar, Cerium oxide nanosheets-based tertiary composites (CeO2/ZnO/ZnWO4) for supercapattery application and evaluation of faradic & non-faradic capacitive distribution by using Donn's model, J Energy Storage. 55 (2022). https://doi.org/10.1016/j.est.2022.105778.
90. M.Z. Iqbal, M.W. Khan, M. Shaheen, S. Siddique, S. Aftab, M. Alzaid, M.J. Iqbal, Evaluation of d-block metal sulfides as electrode materials for battery-supercapacitor energy storage devices, J Energy Storage. 55 (2022). https://doi.org/10.1016/j.est.2022.105418.
91. S. Alam, M.Z. Iqbal, N. Amjad, R. Ali, M. Alzaid, Magnetron sputtered tungsten di-sulfide: An efficient battery grade electrode for supercapattery devices, J Energy Storage. 46 (2022). https://doi.org/10.1016/j.est.2021.103861.
92. Z.Y. Hong, L.C. Chen, Y.C.M. Li, H.L. Hsu, C.M. Huang, Response Surface Methodology Optimization in High-Performance Solid-State Supercapattery Cells Using NiCo2S4–Graphene Hybrids, Molecules. 27 (2022). https://doi.org/10.3390/molecules27206867.
93. Y.Y. How, F. Bibi, A. Numan, R. Walvekar, P. Jagadish, M. Khalid, J. Iqbal, N.M. Mubarak, Fabrication of binary metal phosphate-based binder-free electrode for new generation energy storage device, Surf Coat Technol. 429 (2022). https://doi.org/10.1016/j.surfcoat.2021.127924.
94. M. Roman, S.S.A. Gillani, S. Farid, M. Shakil, R. Ahmad, M.Z. Iqbal, M.M. Faisal, I. Ahmed, S. Alam, Exalted redox frameworks of Cu-MOF/polyaniline/RGO based composite electrodes by integrating silver nanoparticles as a catalytic agent for superior energy featured supercapatteries, Electrochim Acta. 400 (2021). https://doi.org/10.1016/j.electacta.2021.139489.
95. M.Z. Iqbal, J. Khan, Optimization of cobalt-manganese binary sulfide for high performance supercapattery devices, Electrochim Acta. 368 (2021). https://doi.org/10.1016/j.electacta.2020.137529.
96. M.K. Raihana, N. Padmanathan, V. Eswaramoorthi, D. McNulty, J. Sahadevan, P. Mohanapriya, S.E. Muthu, Reduced graphene oxide/VSB-5 composite micro/nanorod electrode for high energy density supercapattery, Electrochim Acta. 391 (2021). https://doi.org/10.1016/j.electacta.2021.138903.
97. M.Z. Iqbal, J. Khan, S. Alam, R. Ali, M.J. Iqbal, A.M. Afzal, S. Aftab, Enhanced electrochemical performance of battery-grade cobalt phosphate via magnetron sputtered copper interfacial layer for potential supercapattery applications, Int J Energy Res. 45 (2021) 18658–18669. https://doi.org/10.1002/er.6974.
98. S. Alam, M.Z. Iqbal, J. Khan, Green synthesis of nickel-manganese/polyaniline-based ternary composites for high-performance supercapattery devices, Int J Energy Res. 45 (2021) 11109–11122. https://doi.org/10.1002/er.6593.
99. M.Z. Iqbal, J. Khan, S. Siddique, A.M. Afzal, S. Aftab, Optimizing electrochemical performance of sonochemically and hydrothermally synthesized cobalt phosphate for supercapattery devices, Int J Hydrogen Energy. 46 (2021) 15807–15819. https://doi.org/10.1016/j.ijhydene.2021.02.077.
100. K. Nasrin, K. Subramani, M. Karnan, M. Sathish, MnCo2S4 – MXene: A novel hybrid electrode material for high performance long-life asymmetric supercapattery, J Colloid Interface Sci. 600 (2021) 264–277. https://doi.org/10.1016/j.jcis.2021.05.037.

101. M.Z. Iqbal, S. Alam, J. Khan, R. Ali, A. Muhammad Afzal, M. Alzaid, S. Aftab, Synergestic effect of magnetron sputtered silver nano-islands and Co3(PO4)2 for high performance supercapattery devices, Journal of Electroanalytical Chemistry. 898 (2021). https://doi.org/10.1016/j.jelechem.2021.115612.
102. M. Alzaid, M.Z. Iqbal, S. Alam, N. Almoisheer, A.M. Afzal, S. Aftab, Binary composites of nickel-manganese phosphates for supercapattery devices, J Energy Storage. 33 (2021). https://doi.org/10.1016/j.est.2020.102020.
103. M.Z. Iqbal, J. Khan, A. Gul, S. Siddique, M. Alzaid, M. Saleem, M.J. Iqbal, Copper doped cobalt-manganese phosphate ternary composites for high-performance supercapattery devices, J Energy Storage. 35 (2021). https://doi.org/10.1016/j.est.2021.102307.
104. T.S. Renani, S.M. Khoshfetrat, J. Arjomandi, H. Shi, S. Khazalpour, Fabrication and design of new redox active azure A/3D graphene aerogel and conductive trypan blue-nickel MOF nanosheet array electrodes for an asymmetric supercapattery, J Mater Chem A Mater. 9 (2021) 12853–12869. https://doi.org/10.1039/d1ta02850b.
105. T. Kavinkumar, S. Seenivasan, A.T. Sivagurunathan, D.H. Kim, Supercapattery driven electrolyzer both empowered by the same superb electrocatalyst, J Mater Chem A Mater. 9 (2021) 21750–21759. https://doi.org/10.1039/d1ta05333g.
106. Y. Li, Z. Luo, S. Liang, H. Qin, X. Zhao, L. Chen, H. Wang, S. Chen, Two-dimensional porous zinc cobalt sulfide nanosheet arrays with superior electrochemical performance for supercapatteries, J Mater Sci Technol. 89 (2021) 199–208. https://doi.org/10.1016/j.jmst.2021.01.085.
107. M. Alzaid, M.Z. Iqbal, S. Siddique, N.M.A. Hadia, Exploring the electrochemical performance of copper-doped cobalt-manganese phosphates for potential supercapattery applications, RSC Adv. 11 (2021) 28042–28051. https://doi.org/10.1039/d0ra09952j.
108. J.J. Zhou, K. Li, W. Wang, Y. Lei, J. Wu, C. Zhou, P. Zhang, J. Liu, Z. Hua, L. Chen, L. Han, Boosting Specific Capacity for Supercapattery by in Situ Formation of Amorphous Ni-Co-Borate on MOF-Derived Ni-Co-LDH Nanosheet Array, ACS Appl Energy Mater. 3 (2020) 12046–12053. https://doi.org/10.1021/acsaem.0c02181.
109. J. Aftab, S. Mehmood, A. Ali, I. Ahmad, M.F. Bhopal, M.Z.U. Rehman, M.Z.U. Shah, A.U. Shah, M. Wang, M.F. Khan, A.S. Bhatti, Synergetic electrochemical performance of tungsten oxide/tungsten disulfide/MWCNTs for high-performance aqueous asymmetric supercapattery devices, J Alloys Compd. 965 (2023). https://doi.org/10.1016/j.jallcom.2023.171366.
110. M. Fawad Khan, M. Ali Marwat, Abdullah, S. Shaheen Shah, M.R. Abdul Karim, M. Abdul Aziz, Z. Ud Din, Saad Ali, K. Muhammad Adam, Novel MoS2-sputtered NiCoMg MOFs for high-performance hybrid supercapacitor applications, Sep Purif Technol. 310 (2023). https://doi.org/10.1016/j.seppur.2023.123101.
111. W. Shehzad, M.R.A. Karim, M.Z. Iqbal, N. Shahzad, A. Ali, Sono-chemical assisted synthesis of carbon nanotubes-nickel phosphate nanocomposites with excellent energy density and cyclic stability for supercapattery applications, J Energy Storage. 54 (2022). https://doi.org/10.1016/j.est.2022.105231.
112. L.G. Ghanem, M.M. Taha, M. Salama, N.K. Allam, Binder-free Mn-V-Sn oxyhydroxide decorated with metallic Sn as an earth-abundant supercapattery electrode for intensified energy storage, Sustain Energy Fuels. (2022). https://doi.org/10.1039/d2se00738j.
113. M. Moradi, M. Mousavi, M. Pooriraj, M. Babamoradi, S. Hajati, Enhanced pseudocapacitive performance of two-dimensional Zn-metal organic framework through a post-synthetic amine functionalization, Thin Solid Films. 749 (2022). https://doi.org/10.1016/j.tsf.2022.139187.
114. M.Z. Iqbal, J. Khan, A.M. Afzal, S. Aftab, Exploring the synergetic electrochemical performance of cobalt sulfide/cobalt phosphate composites for supercapattery devices with high-energy and rate capability, Electrochim Acta. 384 (2021). https://doi.org/10.1016/j.electacta.2021.138358.

115. H. Wu, Z. Qiu, Fe3O4@N-porous carbon nano rice/rGO sheet as positive electrode material for a high performance supercapattery, J Alloys Compd. 879 (2021). https://doi.org/10.1016/j.jallcom.2021.160264.
116. G. Liu, J. Xie, Y. Sun, P. Zhang, X. Li, L. Zheng, L. Hao, G. Shanmin, Constructing 3D honeycomb-like CoMn2O4 nanoarchitecture on nitrogen-doped graphene coating Ni foam as flexible battery-type electrodes for advanced supercapattery, Int J Hydrogen Energy. 46 (2021) 36314–36322. https://doi.org/10.1016/j.ijhydene.2021.08.159.